USGS
science for a changing world

Compositional Analysis of Formation Water Geochemistry and Microbiology of Commercial and Carbon Dioxide-Rich Wells in the Southwestern United States

Scientific Investigations Report 2020–5037

U.S. Department of the Interior
U.S. Geological Survey

Compositional Analysis of Formation Water Geochemistry and Microbiology of Commercial and Carbon Dioxide-Rich Wells in the Southwestern United States

By Jenna L. Shelton, Robert S. Andrews, Denise M. Akob, Christina A. DeVera, Adam C. Mumford, Mark Engle, Michelle R. Plampin, and Sean T. Brennan

Scientific Investigations Report 2020–5037

U.S. Department of the Interior
U.S. Geological Survey

U.S. Department of the Interior
DAVID BERNHARDT, Secretary

U.S. Geological Survey
James F. Reilly II, Director

U.S. Geological Survey, Reston, Virginia: 2020

Suggested citation:
Shelton, J.L., Andrews, R.S., Akob, D.M., DeVera, C.A., Mumford, A.C., Engle, M., Plampin, M.R., and Brennan, S.T., 2020, Compositional analysis of formation water geochemistry and microbiology of commercial and carbon dioxide-rich wells in the southwestern United States: U.S. Geological Survey Scientific Investigations Report 2020–5037, 26 p., https://doi.org/10.3133/sir20205037.

ISSN 2328-0328 (online)

Acknowledgments

We thank Whiting Petroleum Corporation, Kerry Sharer (land owner), and Ray Hartley (land lessee) for allowing access to wells. We thank Yesha Shrestha and Jeanne Jaeschke of the U.S. Geological Survey (USGS) for helpful discussions and laboratory assistance. We thank Christina Kellogg, Nancy Stamm, Bill Orem, Madalyn Blondes, Tina Roberts-Ashby, and Rachel Gidley for thorough and helpful reviews that greatly increased the quality of this work.

Contents

Figures

Tables

Conversion Factors

International System of Units to U.S. customary units

Multiply	By	To obtain
	Length	
nanometer (nm)	3.937×10^{-8}	inch (in.)
micrometer (µm)	3.937×10^{-5}	inch (in.)
centimeter (cm)	0.3937	inch (in.)
meter (m)	3.281	foot (ft)
kilometer (km)	0.6214	mile (mi)
meter (m)	1.094	yard (yd)
	Volume	
microliter (µL)	0.3382×10^{-4}	ounce, fluid (fl. oz)
milliliter (mL)	0.03382	ounce, fluid (fl. oz)
liter (L)	33.81402	ounce, fluid (fl. oz)
liter (L)	2.113	pint (pt)
liter (L)	1.057	quart (qt)
liter (L)	0.2642	gallon (gal)
liter (L)	61.02	cubic inch (in^3)
	Flow rate	
liter per second (L/s)	15.85	gallon per minute (gal/min)
	Mass	
gram (g)	0.03527	ounce, avoirdupois (oz)
kilogram (kg)	2.205	pound avoirdupois (lb)

Temperature in degrees Celsius (°C) may be converted to degrees Fahrenheit (°F) as

$$°C = (°F - 32) / 1.8.$$

Supplemental Information

Concentrations of chemical constituents in water are given in either milligrams per liter (mg/L) or micrograms per liter (µg/L).

Results for measurements of stable isotopes of hydrogen, carbon and oxygen are given in per mil (‰) using delta (δ) notation, as described in the equation:

$$\delta^{18}O = \left(\frac{\left(^{18}O/^{16}O\right)_{sample}}{\left(^{18}O/^{16}O\right)_{standard}} - 1 \right) \times 1000‰$$

Abbreviations

‰	per mil
$CaCO_3$	calcium carbonate
CH_4	methane
clr	centered log-ratio
CO_2	carbon dioxide
CO_3^{2-}	carbonate
CoDA	compositional data analysis
DIC	dissolved inorganic carbon
DNA	deoxyribonucleic acid
EOR	enhanced oil recovery
FeRB	iron-reducing bacteria
GC	gas chromatograph
GMWL	global meteoric water line
H_2S	hydrogen sulfide
HCl	hydrochloric acid
HCO_3^-	bicarbonate
HDPE	high-density polyethylene
ilr	isometric log-ratio
kg/mg	kilogram per milligram
mM	millimolar
N_2	nitrogen gas
NaCl	sodium chloride
NO_2^-	nitrite
NO_3^-	nitrate
NMDS	nonmetric multidimensional scaling
NRB	nitrate-reducing bacteria
OTU	operational taxonomic unit
PC	principal component
PCR	polymerase chain reaction
PO_4^{3-}	phosphate
rRNA	ribosomal ribonucleic acid
SO_4^{2-}	sulfate
SRB	sulfate-reducing bacteria
TDS	total dissolved solids
USGS	U.S. Geological Survey

Compositional Analysis of Formation Water Geochemistry and Microbiology of Commercial and Carbon Dioxide-Rich Wells in the Southwestern United States

By Jenna L. Shelton, Robert S. Andrews, Denise M. Akob, Christina A. DeVera, Adam C. Mumford, Mark Engle, Michelle R. Plampin, and Sean T. Brennan

Abstract

Studies of naturally occurring subsurface carbon dioxide (CO_2) accumulations can provide useful information for potential CO_2 injection projects; however, the microbial communities and formation water geochemistry of most reservoirs are understudied. Formation water and microbial biomass were sampled at four CO_2-rich reservoir sites: two within Bravo Dome, a commercial CO_2 field in New Mexico; one northwest of Bravo Dome in Colorado (Oakdale Field); and one southwest of Bravo Dome in New Mexico (Rafter "K" Ranch). Aside from the Rafter "K" Ranch site, minor differences were observed in the geochemistry of formation water collected from these sites compared to historical data. No organisms were significantly associated with Oakdale Field compared to the other three sites, nor were any hydrogeochemical or gas geochemical parameters (for example, CO_2 concentration) found to have significant associations with the microbial ecology of these four sites. Microorganisms from these sites were metabolically diverse and had the potential to (1) generate methane, (2) produce corrosive hydrogen sulfide (H_2S), and (3) rapidly biofoul and (or) clog pore spaces by shifting microbial communities with changes in salinity or nutrient supply. This study demonstrates that high concentrations of CO_2 in subsurface reservoirs apparently have not imparted a distinct geochemical or microbiological signature on the associated formation waters and that the microorganisms in these reservoirs are metabolically diverse and could adapt to geochemical changes in the subsurface.

Introduction

Geologic carbon sequestration, where carbon dioxide (CO_2) is injected into subsurface formations and retained in porous strata beneath a seal unit, is one method proposed to mitigate rising atmospheric CO_2 concentrations and associated climate change. The first commercial geologic CO_2 sequestration project was initiated in 1996 when the Sleipner CO_2 Storage Facility offshore Norway was brought online. Currently, there are no long-term (more than 100 years) CO_2 sequestration studies, but analogues such as naturally occurring CO_2-rich reservoirs can be studied to examine the biogeochemical processes that may occur during long-term CO_2 storage (for example, Ballentine and others, 2001; Haszeldine and others, 2005; Gilfillan and others, 2009; Sathaye and others, 2014). Many naturally occurring CO_2-rich reservoirs exist across the United States (for example, Allis and others, 2001; Stevens and others, 2001; Stevens, 2005) and have been studied to determine the sources of the emplaced CO_2 (by using stable and noble gas isotopes) and CO_2 storage mechanisms (for example, Gilfillan and others, 2008; Crossey and others, 2009; Zhou and others, 2012; Craddock and others, 2017). To date, only one study has reported on microbial communities from commercial CO_2 reservoirs (Freedman and others, 2017).

The current study is part of a larger study by the U.S. Geological Survey (USGS) to examine natural CO_2 accumulations across the United States in order to gain insight on topics such as sources of naturally occurring CO_2, the effects of high CO_2 concentrations on the geochemistry and microbiology of reservoirs, possible subsurface migration pathways for the CO_2 accumulations, and timing of CO_2 entrainment within traps (for related studies by USGS scientists, see Shelton and others, 2016; Brennan, 2017; and Craddock and others, 2017). Studying CO_2-rich reservoirs is beneficial because they are currently used as sources of CO_2 for enhanced oil recovery (EOR) and could eventually serve as reservoirs for geologic CO_2 sequestration, as they have proven to be capable of trapping large volumes of CO_2 for millions of years. Understanding the microbial communities of CO_2-rich reservoirs is crucial because these microbial populations may affect the fate and transport of injected CO_2 and geologic CO_2 storage mechanisms (for example, Peet and others, 2015). Therefore, understanding how microbial populations and their potential metabolic functions in deep, CO_2-rich subsurface systems adapt to high CO_2 concentrations over long time scales (for example, thousands of years) may help to predict microbial population changes and their effects on potential geologic CO_2 sequestration projects.

The purpose of this study is to delineate the formation water geochemistry and microbial community structures of formations with high CO_2 concentrations to predict possible geochemical and microbiological changes that could occur in various reservoir settings after long-term CO_2 sequestration. It is important to note that no studies to date have analyzed the chemical composition of co-produced water from any commercial CO_2 site, and only one study (Freedman and others, 2017) has analyzed the microbial community composition of co-produced water from a commercial CO_2 site. Therefore, the current study provides a rare opportunity to observe these systems, where there is currently a dearth of data, and to understand how such systems may behave geochemically. We seek to determine whether a particular "microbial signature" is associated with naturally occurring CO_2 reservoirs and to characterize the potential activity of microorganisms in CO_2-rich sites. Furthermore, we examine potential changes in microbial community structure and function that may occur in shallow aquifers in the event of CO_2 leakage from deep sequestration sites.

We collected formation water, microbial biomass, and co-produced gas from four CO_2-rich reservoirs across southeastern Colorado and northeastern New Mexico: two sites in the greater Bravo Dome CO_2 unit region; one in Oakdale Field, northwest of Bravo Dome; and one effervescent shallow groundwater well at Rafter "K" Ranch, southwest of Bravo Dome. For more information on these sites, readers are referred to Brennan (2017). To our knowledge, these are the first formation water and microbial samples collected from the Bravo Dome unit. Although we collected a small number of samples, studying these sites, where large volumes of relatively pure CO_2 are produced from the subsurface, and similar CO_2 accumulations across the United States can provide more insight into how high CO_2 concentrations could affect microbial communities and formation water geochemistry (and thus, possibly affect geologic CO_2 sequestration) in large-scale, permanent CO_2 injection sites.

Background and Study Sites

Bravo Dome

Two water samples were collected from producing wells associated with the West Bravo Dome CO_2 exploration unit, a large commercial CO_2 field in northeastern New Mexico (fig. 1). The gas produced from Bravo Dome was historically used to produce dry ice (Johnson, 1983) and now is primarily piped to the Permian Basin and used for CO_2-EOR operations. Most of the CO_2 produced from Bravo Dome is sourced from Permian strata, specifically the Abo Formation and the Tubb sandstone (basal unit of the Yeso Formation); small volumes of CO_2 are also produced from the Triassic Santa Rosa Formation (after Broadhead, 1990). The Abo-Tubb strata are eolian and fluvial sandstones containing discrete intervals of dolomitic paleosols with high concentrations of manganese, low strontium and sodium concentrations, and variable iron content (Hartig and others, 2011). The Triassic Santa Rosa Formation was subdivided into three members by Lucas and Hunt (1987): the Tecolotito Member, the Los Esteros Member, and the Tres Lagunas Member. The Tres Lagunas Member is the uppermost and most described member of the Santa Rosa and is a predominantly orange and yellowish-brown, medium-grained quartzarenite sandstone. Stratigraphically below the Tres Lagunas is the Los Esteros Member, a yellow and reddish-brown mudstone with intervals of very fine- to fine-grained quartzarenite sandstone. The Tecolotito Member has a basal limestone-cobble conglomerate, and the overlying rocks are grayish-orange to pale-orange, laminated and crossbedded, medium-grained quartzarenite.

Bravo Dome has been studied because of the large volume of CO_2 emplaced in the subsurface there; studies have included analyzing the long-term effects of CO_2 sequestration in saline aquifers (Gilfillan and others, 2009; Hartig and others, 2011), estimating the timing of CO_2 emplacement in the dome (Gilfillan and others, 2008; Broadhead and others, 2009), delineating the current CO_2 flux into the reservoir (Baines and Worden, 2004; Sathaye and others, 2014; Brennan, 2017), and analyzing the system's suitability as a target and (or) analogue reservoir for geologic CO_2 sequestration (Rochelle and others, 1999; Allis and others, 2001; Stevens and others, 2001; Gilfillan and others, 2009). Despite the numerous studies of Bravo Dome, no data on either co-produced waters or subsurface microbiology have been published. Previous research suggested that the main CO_2-producing reservoir of Bravo Dome, the Permian Tubb sandstone, is hydrologically sealed and that producing regions of the reservoir are compartmentalized and therefore hydrologically disconnected from adjacent reservoirs (Akhbari and Hesse, 2017). If the Tubb sandstone is compartmentalized in northeastern New Mexico, the formation water geochemistry of Bravo Dome may deviate from regional trends. Furthermore, producing wells across Bravo Dome may be geochemically different if they produce from different compartmentalized regions.

Oakdale Field

Oakdale Field is a gas-producing field within the Raton Basin in Huerfano County, Colorado, northwest of Bravo Dome. The main reservoirs of Oakdale Field are the Jurassic Entrada Sandstone and the Cretaceous Dakota Sandstone that, in addition to natural gas, produce large volumes of CO_2. The Entrada Sandstone is a fine- to coarse-grained, parallel-bedded, white to pink and red, well-sorted sandstone with mostly rounded and frosted quartz grains (Baltz, 1965). Chert and feldspar grains are also present in the sandstone, and the sandstone's cement is typically calcareous and, in some places, gypsiferous (Baltz, 1965). The Dakota Sandstone in this area is gray to buff colored and interbedded with gray shale. Lenses

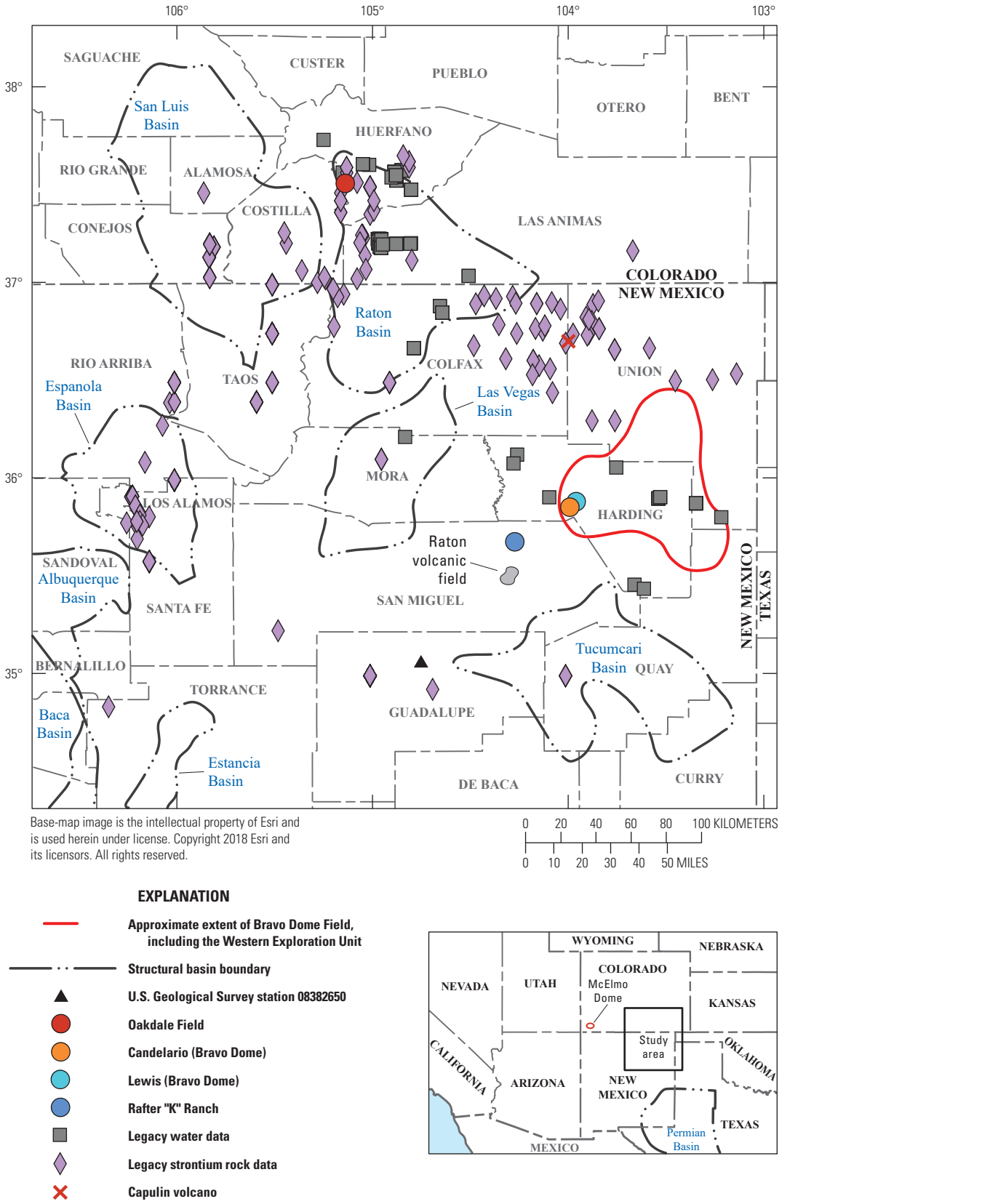

Figure 1. Map showing sample sites and locations of legacy data (U.S. Environmental Protection Agency, 2016; Blondes and others, 2018; EarthChem, 2018; Petroleum Recovery Research Center, 2018; U.S. Geological Survey, 2018).

of conglomerate, as well as areas of pure sandstone, are common in the western part of the Raton Basin (Baltz, 1965). The Dakota Sandstone is loosely cemented and well sorted in some areas, and in other areas it is fine grained to finely conglomeratic (Baltz, 1965) and has a lenticular, nonmarine shale at its base (Owen, 1966). These two sandstones also produce large volumes of CO_2 from other areas of southeastern Colorado, such as Sheep Mountain and Dike Mountain Fields (Roth, 1983; Worrall, 2004). The third producing (gas only as of 2004) reservoir is a felsite dike, emplaced as a magmatic fluid, with primary and fracture porosity. The felsitic section has historically produced mostly methane (CH_4) with complementary volumes of CO_2 (15–20 percent; Worrall, 2004).

These sandstone producing formations typically have double the average porosity of rocks in the Raton Basin (Worrall, 2004). This high porosity is likely due to a lack of silicification caused by lack of recharge; silicification has been identified in other areas of the basin and attributed to active recharge (Worrall, 2004). Historically, wells in Oakdale Field have produced gas with a CO_2 content ranging from 24 to 97 percent on average, with the remainder of the gas typically dominated by hydrocarbons (for example, ethane; Worrall, 2004). In 2016, nine wells were producing from Oakdale Field, specifically from the Entrada and Dakota Sandstones and the Cretaceous Pierre Shale (Colorado Oil and Gas Conservation Commission, 2018).

Rafter "K" Ranch

The Rafter "K" Ranch is in San Miguel County, New Mexico, approximately 15 kilometers southwest of the greater West Bravo Dome CO_2 exploration unit (Brennan, 2017). The samples collected for this study originated from a shallow (47.25 meters [m] deep), nonpumping groundwater well, which began effervescing CO_2 upon completion of the well (Ray Hartley, oral commun., 2015). The well is drilled into exposed Triassic strata, similar to that of the West Bravo Dome CO_2 exploration unit; Brennan (2017) hypothesized that the well is, like Bravo Dome, producing from the Santa Rosa Formation. The well was sampled to determine if the produced CO_2 had a source similar to that of the CO_2 produced from Bravo Dome (Brennan, 2017) and to assess the long-term microbial and geochemical effects of a CO_2 leak into a shallow aquifer.

Methods

Field Sampling

During sampling campaigns in June 2015 and August 2016 (table 1, fig. 1), we collected formation waters at the four sites for chemical and microbiological analyses. Co-produced gases were also collected, and methods for this work can be found in Brennan (2017). Samples came from the Candelario well and the Lewis well in Bravo Dome, the Oakdale Field water storage tank, and the Rafter "K" Ranch water well (fig. 1). Although low volumes of water were produced, water was collected directly from the Candelario and Lewis wellheads into sterile 2-liter (L) glass bottles. The Oakdale Field water was collected from a water storage tank that was open to the atmosphere and contained a mixture of produced water from all nine wells within the field. Water was obtained from the Rafter "K" Ranch groundwater well by using a Geocontrol PRO bladder pump (Geotech Environmental Equipment, Inc., Denver, Colorado) after purging at a rate of 6.3 liters per hour for 2 hours. Solid material from these producing formations could not be obtained to analyze biofilms or organisms present on the surfaces. Sterile plastic Nalgene tubing was inserted into each bottle, once filled with sample water, and was attached to a 0.22-micrometer (μm) Sterivex GP filter unit using a peristaltic pump. Water was pumped through the filter until the filter clogged, and the filter was immediately stored on dry ice. The remaining water was filtered according to the geochemical analysis protocol listed below and collected into high-density polyethylene (HDPE) or glass sample bottles (major and minor geochemistry and isotopes), preserved according to the analysis protocol, and stored immediately on ice. Unfiltered water was also collected in anoxic (nitrogen gas [N_2] headspace) 120-milliliter (mL) glass serum bottles for microbial cultivation. Each serum bottle was filled with approximately 60 mL of produced water.

All samples collected for trace element and cation analysis were filtered at 0.45 μm and acidified to a pH below 2 using Optima-grade nitric acid; samples collected for the analysis of anions, alkalinity, and total dissolved solids (TDS) were simply filtered using a 0.45-μm filter unit. Water for stable hydrogen and oxygen isotopes of water (δ^2H and $\delta^{18}O$) and strontium isotope (strontium-87/strontium-86 [$^{87}Sr/^{86}Sr$]) analysis was filtered at 0.45 μm with a Geotech Environmental Equipment, Inc. capsule filter. All water sample bottles were filled (leaving no headspace), stored on ice, and shipped to the USGS in Reston, Virginia, where they were stored at 4 degrees Celsius (°C) until analysis. All Sterivex GP filter units for microbial community analysis were shipped on dry ice to the USGS where they were held at −80 °C until shipment to Jonah Ventures (Boulder, Colorado) for sample analysis. A field blank was collected for each analysis (for example, cations) as a quality-control check. The blanks for water samples were 18-megaohm water collected following filtering and preservation methods for a given sample type (for example, cations). The blanks for the Sterivex filters were prepared by passing 2 L of 18.2-megaohm-centimeter water through a Sterivex GP filter unit.

Table 1. Summary of study sites and samples collected.

[API, American Petroleum Institute; NA, not applicable]

Site	Sample date	API number	Geologic formation	State (county)	Coordinates	Lower depth, in meters	Sample type
Lewis (Bravo Dome)	6/15/2015	30-012-20587	Santa Rosa Formation and Tubb sandstone	New Mexico (Harding)	35.904125, −103.93255	1,067	Water chemistry and microbial sequencing
Candelario (Bravo Dome)	5/15/2015	30-021-20659	Santa Rosa Formation and Tubb sandstone	New Mexico (Harding)	35.88815, −103.950342	1,158	Water chemistry and microbial sequencing
Oakdale Field	8/15/2016	NA	Pierre Shale, Dakota Sandstone, and Entrada Sandstone	Colorado (Huerfano)	37.539059, −105.104617	1,720*	Water chemistry, microbial sequencing, and cultivation
Rafter "K" Ranch	6/10/2015; 8/18/2016	NA	Triassic strata and Santa Rosa Formation	New Mexico (San Miguel)	35.705738, −104.238507	47	Water chemistry, microbial sequencing, and cultivation

*Average depth of producing wells from Oakdale Field.

Analytical Methods for Geochemical and Isotopic Analysis

Produced water temperature (not indicative of downhole temperature), conductivity, and pH were measured in the field immediately after water collection by using a Thermo Scientific Orion Star A325 portable pH/conductivity/temperature multiparameter meter kit with an Orion ROSS Triode pH/automatic temperature compensation (ATC) gel-filled electrode and an Orion DuraProbe conductivity cell. Stable isotopes of water—δ^2H-H_2O and δ^{18}O-H_2O—were measured to a precision of ±2.0 per mil (‰) and ±0.3 ‰, respectively, by Isotech Laboratories, Inc. in Champaign, Illinois. The δ^{13}C of dissolved inorganic carbon (DIC) in water was measured to a precision of ±0.2 ‰ by Isotech Laboratories, Inc. in Champaign, Illinois. Anions and trace metals were measured by Activation Laboratories Ltd. in Ancaster, Ontario, Canada. Anions were measured by using a Dionex DX-120 ion chromatograph system, and trace metals were analyzed by inductively coupled plasma-optical emission spectroscopy (ICP-OES) on an Agilent Axial 730-ES (emission spectrometer), with detection limits varying for the measured elements (table 2). Field blanks for both anions and trace metals contained negligible amounts of the measured elements (that is, below laboratory detection limits). Charge balance errors ranged from −14.2 to 15.4 percent and did not include a direct measurement of DIC (only alkalinity) or the dissolved organic composition constituents, as they were not measured.

Strontium isotopes were measured on a Nu Plasma multiple-collector inductively coupled plasma mass spectrometer at the Center for Earth and Environmental Isotope Research at the University of Texas at El Paso after column separation in a class-100 clean room. Samples were purified by using Eichrom Technologies Inc. strontium resin, dried down, and brought up in 2 percent nitric acid. Strontium isotope ratios were corrected on-line for any interferences with krypton (Konter and Storm, 2014). Accuracy was acceptable, as shown through the average result of 0.70918 for the secondary standard USGS EN-1 versus the accepted value of 0.709174. External error (2s) was 0.000023 on the basis of variation in the USGS EN-1 standard (n=5) over the 2 days of analysis. Field blanks contained negligible amounts of strontium (less than 100 millivolts).

To increase the robustness of the dataset and to compare the samples from this study to other data from the region, produced water data from similar strata in Colorado and New Mexico were obtained from a variety of external databases and literature. Data were selected if they were from the same county as any of the four samples collected in this study (Huerfano County, Colorado; Harding County, New Mexico; and San Miguel County, New Mexico), the Las Vegas Basin, or the Raton Basin, or were within these general regions and contained relevant data (for example, ^{87}Sr/^{86}Sr values). External data sources included the USGS National Produced Waters Geochemical Database version 2.3 (https://doi.org/10.5066/F7J964W8; Blondes and others, 2018), the USGS National Water Information System (https://nwis.waterdata.usgs.gov/nwis; U.S. Geological Survey, 2018), a U.S. Environmental Protection Agency study on hydraulic fracturing (U.S. Environmental Protection Agency, 2016), and the New Mexico Produced Water Quality Database version 2 (http://gotech.nmt.edu/gotech/Water/producedwater.aspx; Petroleum Recovery Research Center,

Table 2. Field-measured water-quality parameters, concentrations of ions and trace elements, and isotopic composition of produced fluids.

[Total dissolved solids (TDS) includes the sum of trace ions that were measured but not presented in this table. Dissolved inorganic carbon (DIC) and dissolved organic carbon were not measured and could not be included in the TDS sum. The laboratory detection limits for the analytes were as follows: sodium (Na^+), 5 micrograms per liter (µg/L); potassium (K^+), 30 µg/L; calcium (Ca^{2+}), 700 µg/L; magnesium (Mg^{2+}), 2 µg/L; strontium (Sr), 0.04 µg/L; silicon (Si), 200 µg/L; iron (Fe), 10 µg/L; chloride (Cl^-), 30 µg/L; bromine (Br^-), 30 µg/L; nitrate (NO_3^-) as nitrogen (N), 10 µg/L; nitrite (NO_2^-) as N, 10 µg/L; phosphate (PO_4^{3-}) as phosphorus (P), 20 µg/L; and sulfate (SO_4^{2-}), 30 µg/L. °C , degree Celsius; NA, not measured or not available; mg/L, milligram per liter; $CaCO_3$, calcium carbonate; <, a precise concentration could not be generated because the sample was diluted and close to the laboratory detection limit; $^{87}Sr/^{86}Sr$, strontium-87/strontium-86; ‰, per mil; CO_2, carbon dioxide; %, percent; CH_4, methane; Ar, argon; ND, not detected; He, helium; C_{2+}, hydrocarbons measured in the gas with greater than or equal to two carbon atoms]

Parameter	Units	Sample			
		Candelario (Bravo Dome)	Lewis (Bravo Dome)	Oakdale Field*	Rafter "K" Ranch
Temperature	°C	NA	NA	25.3	32.5
pH	Unitless	7.2	6.6	6.5	6.4
Alkalinity	mg/L as $CaCO_3$	5,446	1,575	15,737	10,825
Na^+	mg/L	11,300	8,880	19,000	63
K^+	mg/L	127	62	123	25
Ca^{2+}	mg/L	2,200	3,560	358	573
Mg^{2+}	mg/L	2,650	540	102	127
Sr	mg/L	41.2	59.6	37.5	50.6
Si	mg/L	35.2	65.6	33.3	7.1
Fe	mg/L	100	112	35	5
Cl^-	mg/L	15,200	15,900	16,000	19
Br^-	mg/L	46.2	46.5	91.4	<0.3
NO_2^- (as N)	mg/L	<2.0	<2.0	<2.0	<0.1
NO_3^- (as N)	mg/L	3.2	2.1	<2.0	<0.1
PO_4^{3-} (as P)	mg/L	<3.0	<3.0	<3.0	<0.2
SO_4^{2-}	mg/L	3,340	1,750	577	573
TDS	mg/L	31,013	31,013	36,426	1,400
$^{87}Sr/^{86}Sr$	Unitless	0.72421	0.72899	0.70855	0.70856
$\delta^{18}O\text{-}H_2O$	‰	−9.04	−9.22	0.03	−7.01
$\delta^{2}H\text{-}H_2O$	‰	−62.5	−62.4	−17.5	−47.7
$\delta^{13}C\text{-}DIC$	‰	3.4	1.7	2.3	0.3
CO_2	%	99.5	99.8	76.2	99.5
CH_4	%	0.002	0.001	18.758	0.001
Ar	%	0.008	ND	0.024	0.007
He	%	0.027	0.020	0.047	0.008
C_{2+}	%	ND	ND	3.76	ND

*Value is the average mole percent of gas components (standard deviation = 28.0) in wells that produce from Oakdale Field (*n*=7).

2018). These data are hereafter referred to as the "legacy water samples," and they include water from multiple surface-water sites, monitoring wells, domestic water wells, and production wells, as well as time-series data from many of these sites. Furthermore, additional outside data concerning hard-rock strontium concentrations and isotopic values ($^{87}Sr/^{86}Sr$) were compiled for the study region from the EarthChem Portal (http://www.earthchem.org/portal; EarthChem, 2018).

Characterization of Microbial Community Composition

Deoxyribonucleic acid (DNA) extractions, amplifications, and Illumina MiSeq 16S ribosomal ribonucleic acid (rRNA) gene sequencing were completed by Jonah Ventures in Boulder, Colorado. Following Jonah Ventures protocol, DNA was extracted by opening the Sterivex GP filter units

and vigorously swabbing the entire surface of the filter with a clean sterile swab. This method was performed to reduce contamination induced by slicing the filter and to obtain the entire community present on the filter, as using slices of filter might not capture communities present on unused portions (for examples of this method, see Grice and others, 2008; Ramirez and others, 2014; Barberán and others, 2015; Leff and others, 2015; Luongo and others, 2016). The swab was then used for extraction in the MO BIO Laboratories, Inc. (Carlsbad, California) PowerSoil-htp 96-Well DNA isolation kit following the manufacturer's given protocol. For quality-control purposes, eight extraction blanks and two swab blanks were included in the dataset.

Following extraction, the V4 region of the 16S rRNA gene was amplified by using the 515F (5' – GTGYCAGC-MGCCGCGGTAA – 3') and 806R (5' – GGACTAC-NVGGGTWTCTAAT – 3') primer pair (Apprill and others, 2015; Walters and others, 2015; Parada and others, 2016). Both primers included 5' Illumina adaptor sequences to allow for indexing and sequencing. Polymerase chain reaction (PCR) was performed by using the Promega PCR Master Mix (Promega Corp. catalog no. M5133; Madison, Wisconsin) according to the manufacturer's protocol, using the primers (both 0.2 micromolar [µM]) and 1 microliter (µL) of sample DNA. The following conditions were used for the first PCR amplification: initial denaturation at 95 °C for 5 minutes (min), followed by 35 cycles for 45 seconds (s) of denaturation at 95 °C, annealing for 60 s at 50 °C, extension for 90 s at 72 °C, and a final elongation at 72 °C for 10 min. Unincorporated single-stranded DNA and DNA polymerase were removed from PCR products by incubating the amplicons with Exo1/SAP (Shrimp Alkaline Phosphatase) for 30 min at 37 °C, followed by an inactivation step at 95 °C for 5 min. A second round of PCR was performed to incorporate a unique 12-nucleotide index sequence into each sample. The indexing PCR included the primers (0.5 µM each), Promega PCR Master Mix, and 2 µL of template DNA (that is, the cleaned amplicon from the first PCR reaction). Initial denaturation was at 95 °C for 3 min, followed by eight cycles for 30 s at 95 °C, annealing at 55 °C for 30 s, and extension at 72 °C for 30 s. After both PCR reactions, 5 µL of PCR products from each sample was normalized and cleaned using SequalPrep Normalization Plates (Life Technologies Corp., Carlsbad, California). The samples were then pooled together for sequencing on an Illumina MiSeq (Illumina, Inc., San Diego, California) at the University of Colorado Boulder BioFrontiers Sequencing Facility, running 1 x 150 base pair chemistry and using the v2 300-cycle kit (Illumina Inc. catalog no. MA-102-2002).

QIIME 2 version 2017.11 (Caporaso and others, 2010; www.qiime2.org) was used for downstream processing. The data were processed following the protocol outlined in the "Moving Pictures" tutorial (QIIME 2 Development Team, 2017; https://docs.qiime2.org/2017.11/tutorials), with some modifications. Sequences were trimmed and truncated where the quality score dropped below 30 by using the DADA2 plugin of QIIME 2 (--p-trim-left 14; --p-trunc-len 150). Phylogenetic classification was performed by using a Naive Bayes classifier trained on the SILVA 119 database within QIIME 2 (QIIME 2 Development Team, 2018; https://docs.qiime2/org/2018.4/data-resources/) (Pruesse and others, 2007; Quast and others, 2013), and the following parameters were modified: --p-pre-dispatch 1, --p-chunk-size 1000.

The final data were read into R version 3.3.3 (R Core Team, 2017) for all additional downstream processing steps and statistical analyses. Sequences matching chloroplast phylotypes were removed. The operational taxonomic units (OTUs) identified at greater than 1-percent abundance in the blanks (28 OTUs) were removed from the sample set to reduce contamination (for example, Salter and others, 2014), and the samples were rarefied to 24,000 sequences per sample. Sequence reads for each sample were deposited in the National Center for Biotechnology Information Sequence Read Archive under BioProject PRJNA470686 and BioSample accession numbers SRR7140487–SRR7140489. Data and associated metadata are available in Shelton, DeVera, and others (2018).

Cultivation of Microbial Functional Groups

Microbial functional groups were cultured from the Rafter "K" Ranch and Oakdale Field water samples in anaerobic media selective for six microbial functional groups at three sodium chloride (NaCl) salinities (freshwater, 1 gram per liter [g/L]; seawater, 20.0 g/L; and brine, 100 g/L) and at two CO_2 concentrations (20 percent and 100 percent) for a total of 36 cultivation conditions. A broad range of salinities were tested to provide a proxy for geochemical changes that could result from mixing of high- and low-salinity waters in aquifers. In addition, by testing multiple salinities, we aimed to provide information on the range of salinity tolerated by the native microbial communities. Two CO_2 concentrations were tested to evaluate the microbial response to various CO_2 concentrations because CO_2 concentrations could vary in situ.

The microbial functional groups targeted included CO_2 fixers and hydrogenotrophic methanogens (autotrophs), iron-reducing bacteria (FeRB), acetoclastic methanogens (methanogens), nitrate-reducing bacteria (NRB), sulfate-reducing bacteria (SRB), and heterotrophs/fermenters (heterotrophs). The functional groups tested were chosen to evaluate (1) microbial responses to inputs of deep or shallow waters with varying geochemical conditions and (2) the potential activity of microorganisms in a CO_2 sequestration analogue.

An anoxic, sterile, bicarbonate-buffered mineral media (modified from Widdel and Bak, 1992; pH 7) was used as the base media for enrichment cultures. Per liter, freshwater media contained the following: 0.4 gram (g) magnesium chloride $(MgCl_2)\cdot 6H_2O$, 0.1 g calcium chloride $(CaCl_2)\cdot 2H_2O$, 0.3 g ammonium chloride (NH_4Cl), and 0.6 g monopotassium phosphate (KH_2PO_4). Each liter of seawater and brine media

contained 3.0 g $MgCl_2 \cdot 6H_2O$, 0.15 g $CaCl_2 \cdot 2H_2O$, 0.25 g NH_4Cl, and 0.2 g KH_2PO_4. Per liter, all media contained 0.5 g potassium chloride (KCl), 3.2 g sodium bicarbonate ($NaHCO_3$), 1 mL of trace element solution SL-9 (Tschech and Pfennig, 1984), and 1 mL of 0.1 percent resazurin solution as redox indicator. Media (10 mL) was dispensed under 80/20 N_2/CO_2 into Balch pressure tubes containing approximately 0.7 g of 0.5-mm glass beads, which were added to act as an inert surface for microbial growth. The tubes were capped with butyl rubber stoppers (Bellco Glass Inc.) and aluminum crimp seals and then autoclaved at 121 °C for 20 min. After autoclaving, media was amended with 1 milliliter per liter Wolfe's vitamin solution (Zeikus and others, 1983), selenite-tungstate solution (the final concentration in media was 1 µM Na_2SeO_3 and $Na_2WO_4 \cdot 2H_2O$), and cysteine-sulfide reductant (Zeikus and others, 1983) from sterile, anoxic stocks. Enrichment cultures for NRB and FeRB also contained 0.5 millimolar (mM) iron chloride ($FeCl_2$) as reductant.

Media were further amended with electron acceptors and donors to selectively enrich for the six microbial functional groups. The final concentrations of amendments were as follows: (1) autotrophs—approximately 0.001 percent yeast extract and 10 mL hydrogen gas (H_2); (2) heterotrophs—6.4 g/L Bacto Peptone (Difco Laboratories), 1.1 g/L yeast extract, and 8.5 g/L glucose; (3) FeRB—approximately 50 mM amorphous iron oxide (FeOOH), 4 mM citrate, 4 mM acetate, and 4 mM lactate; (4) NRB—200 mM glycerol and 50 mM sodium nitrate ($NaNO_3$); (5) SRB—citrate, acetate, and lactate, all 4mM, and 20 mM sodium sulfate ($NaSO_4$); and (6) methanogens—13 mM acetate. Amorphous FeOOH was synthesized according to the method of Lovley and Phillips (1986). Prior to inoculation, pressure tubes were briefly flushed by using aseptic technique with 80/20 N_2/CO_2 or 100 percent CO_2 for low- or high-CO_2 conditions, respectively, and left overpressured. Cultures were inoculated with 1 mL of water sample. A sterile control was prepared for each experimental combination by omitting the inoculant. Pressure tubes were incubated in the dark at 37 °C while shaking at 75 rotations per minute.

Cultures were visually monitored for approximately 5 weeks and scored at least weekly. Scoring consisted of a subjective scale from negative to four-plus based on turbidity and any other changes in appearance that indicated biological activity. Geochemical analyses were performed to confirm visual observations. The NRB culture samples were filtered (0.22-µm Supor filters), then nitrate concentrations were determined by ion chromatography using a Dionex ICS-1000 ion chromatograph with an ED50 electrochemical detector and a high-capacity AS14 anion-exchange column. Sulfate reduction by SRBs was verified by using lead acetate strips (Fisher Scientific), where a dark color change indicated H_2S production. Dissolved divalent iron (Fe[II]) concentrations in FeRB cultures were determined by extracting samples in 0.5-molar hydrochloric acid (HCl) for 1 hour. The HCl-extractable Fe(II) in extracts was quantified colorimetrically by analysis in ferrozine buffer: 50-mM 4-(2-hydroxyethyl)-1-piperazineethanesulfonic acid (HEPES), 0.1 percent ferrozine, pH 7 (Kostka and Luther, 1994). Absorbance was measured at 562 nanometers and converted to iron concentrations on the basis of a standard curve of known Fe(II) concentrations.

Methane was measured in methanogen, autotroph, and heterotroph cultures by using a gas chromatograph (GC) with thermal conductivity detection. Samples were collected from culture tubes by using a sampling valve and 1-mL pressure-lock, tight syringes (Valco Instruments Co. Inc.) with non-coring needles. The sampling valve consisted of a Hamilton HV plug valve (Hamilton Co., Reno, Nevada), sealed with Thermogreen LB-2 5-mm septa (Supelco, Inc., Bellefonte, Pennsylvania), and Kel-F female and male luer fittings (Hamilton Co. no. 35031 and no. 35030). A sterile syringe needle was attached to the male end and then inserted into the flamed stopper of a microcosm bottle. Using a pressure lock syringe, 0.2 mL of gas was removed and injected into a Hewlett Packard 6890 series GC (GMI Inc.). Separation was performed using a HayeSep N 80/100 mesh column with a 3-m, 1/8-inch Nafion dryer. The GC operated with nitrogen as the carrier gas (20 milliliters per minute [mL/min] total flow); temperatures of 40 °C, 155 °C, and 180 °C for the oven, injector, and detector, respectively; and an injector flow rate of 20 mL/min total flow. The GC signals were analyzed with VP CLASS 7.3 software (Shimadzu, Columbia, Maryland). Instrument responses were calibrated with CH_4 standards (Scott Specialty Gases, Plumsteadville, Pennsylvania). A GMH 3111 digital pressure meter with a GMSD needle pressure transducer (Greisinger Electronic GmbH, Germany) was used to measure gas pressure in culture tubes. Methane concentrations measured by the GC in parts per million were converted to micromoles of CH_4 gas in headspace by using the Ideal Gas Law (eq. 1).

$$\frac{(P_{atm} + P_{HS}) \times V_{HS}}{R(T + 273.15)} \times \frac{X_{CH_4}}{10^6} = n_{CH_4} \quad (1)$$

where

P_{atm} is the room pressure in millibars;
P_{HS} is the headspace overpressure in millibars;
X_{CH_4} is the concentration of methane in headspace in parts per million;
V_{HS} is the headspace volume in milliliters;
R is the ideal gas constant (8.314×10^4 milliliter millibar per mole per degree kelvin); and
T is the laboratory temperature in degrees Celsius.

Compositional Data Analysis

Chemical data from waters are typically measured and statistically analyzed as concentrations of specific elements (for example, as milligrams per liter, millimoles per liter, and so on). Water-chemistry datasets, however, are fundamentally compositional (Lovell and others, 2011; Engle and Rowan,

2013, 2014) and require particular mathematical treatment to successfully interpret the data. Many issues with data interpretation, such as spurious relations or misleading conclusions, have been noted when using standard mathematical and statistical techniques on ion and elemental data, particularly in brines (for example, Aitchison, 1986; Buccianti and Pawlowsky-Glahn, 2005; Engle and Rowan, 2013, 2014; Engle and Blondes, 2014). Therefore, we used methods of compositional data analysis (CoDA) to analyze the subcompositions of the nonisotopic chemical data. These methods were created to avoid and overcome issues surrounding traditional water-quality assessment methods and plotting techniques (for example, Piper plots). For an in-depth explanation of CoDA, as well as the centered log-ratio (clr) and isometric log-ratio (ilr) transformations, we refer readers to fundamental papers (Aitchison, 1986; Egozcue and others, 2003; Pawlowsky-Glahn and Buccianti, 2011; Engle and Rowan, 2013).

Produced Fluid Geochemistry

Produced water was collected from four sites during the two sampling campaigns (table 1). In this section, Rafter "K" Ranch results are highlighted individually because of the difference in setting compared to the other sites (shallow groundwater versus deep hydrocarbon environments). The water temperature was 25.3 °C at Oakdale Field and 32.5 °C at Rafter "K" Ranch; water temperature was not recorded at Candelario and Lewis wells (Bravo Dome samples). The pH of the samples ranged from 6.4 (Rafter "K" Ranch) to 7.2, and alkalinity ranged from 1,575 milligrams per liter (mg/L) as calcium carbonate ($CaCO_3$) to 15,737 mg/L as $CaCO_3$ (10,825 mg/L as $CaCO_3$ at Rafter "K" Ranch). Sodium (Na^+) concentrations ranged from 63 mg/L (Rafter "K" Ranch) to 19,000 mg/L, and chloride (Cl^-) concentrations ranged from 19 mg/L (Rafter "K" Ranch) to 16,000 mg/L. Calcium (Ca^{2+}) concentrations ranged from 358 to 3,560 mg/L (573 mg/L at Rafter "K" Ranch), magnesium (Mg^{2+}) concentrations ranged from 102 to 2,650 mg/L (127 mg/L at Rafter "K" Ranch), and sulfate (SO_4^{2-}) concentrations ranged from 573 (Rafter "K" Ranch) to 3,340 mg/L (table 2). Most concentrations of nitrite (NO_2^-) (as nitrogen [N]), nitrate (NO_3^-) (as N) and phosphate (PO_4^{3-}) (as phosphorus [P]) were at or below laboratory detection limits. Produced gas data and results are described in Brennan (2017) and can be found in table 2.

Figure 2 is a covariance clr biplot that allows for interpretation of the variance of different ratios of cations and anions across the study area. When interpreting a clr biplot, it is most important to analyze the position and length of the links between the rays instead of simply the size and direction of the rays themselves. Principal component (PC) 1 explains a majority of the variance in the dataset, 84.5 percent, and PC1 and PC2 combined explain almost all of the variance present in the dataset (95.8 percent total). The links between concentrations of Mg^{2+} and Na^++ potassium (K^+), Mg^{2+} and Cl^-, and Mg^{2+} and SO_4^{2-} are all subparallel to PC1, meaning that PC1 reflects variation in the ratios $Mg^{2+}/Na^+{+}K^+$, Mg^{2+}/Cl^-, and Mg^{2+}/SO_4^{2-} across the sample set. Almost all links from DIC to the other elements are subparallel to PC2, meaning that PC2 explains the variation in DIC concentrations across the sample sites. Short links between concentrations of $Na^+{+}K^+$ and Cl^- and Cl^- and SO_4^{2-} suggest that these constituents occur proportionally and may be associated with each other across the studied region. The fact that PC1 explains most variance in the dataset suggests that most of the variance is due to differences in $Na^+{+}K^+$, Cl^-, and SO_4^{2-} concentrations compared to Mg^{2+} concentrations across the dataset.

The ilr-ion plot is a CoDA alternative to the Piper diagram that shows ilr-transformed concentrations of major cations and anions, similar to a Piper diagram (the ilr-ion plot is described fully in Shelton, Engle, and others, 2018). Most water samples in the current study (4 original samples and 108 legacy samples from other sources) are $Na^+{+}K^+$ type (lower left panel of fig. 3), with variation in the dominating anion (upper right panel of fig. 3). Minimal clustering of samples is apparent, meaning that, in general, the current and legacy water samples tend to be geochemically diverse. The clusters that do appear are samples that were collected as time-series data from the same location or samples from similar stratigraphic settings (U.S. Environmental Protection Agency, 2016). The Bravo Dome samples are generally similar in that both are $Na^+{+}K^+$- and Cl^--type waters. The water produced from the Lewis well, however, has a greater Ca^{2+} concentration than Mg^{2+} concentration, whereas the Candelario well sample has a greater Mg^{2+} concentration than Ca^{2+} concentration (left panels of fig. 3). The Rafter "K" Ranch sample is the most dissimilar of the four CO_2-rich reservoir samples collected, with water produced being Ca^{2+} and bicarbonate (HCO_3^-)+carbonate (CO_3^{2-}) type.

The four water samples collected for this study are, in general, isotopically similar to regional waters, in that all appear to be of meteoric origin (fig. 4). The current data and the legacy water data, in general, fall near the global meteoric water line (GMWL; Craig, 1961) and the local meteoric water line (LMWL; developed for the Pecos River above Santa Rosa Lake, New Mexico; USGS station number 08382650; Coplen and Kendall, 2000). The samples collected in the current study generally have more enriched δ^2H-H_2O and $\delta^{18}O$-H_2O values than the legacy data, with the Oakdale Field and Rafter "K" Ranch samples being obvious outliers (fig. 4). These isotopic differences in the Rafter "K" Ranch and Oakdale Field samples compared to the other samples in the dataset may be due to differences in recharge temperatures, the CO_2-rich condition of the reservoirs, or evaporation during recharge (the Oakdale Field sample may have been affected by evaporation while in the storage tank). For example, three evaporation scenarios are plotted in figure 4, showing how the isotopic composition of water could shift during evaporation at 25, 50, and 75 percent humidity. Oxygen exchange is an expected isotopic deviation for waters in high-CO_2 environments, meaning oxygen-16 from the in situ CO_2 would preferentially exchange

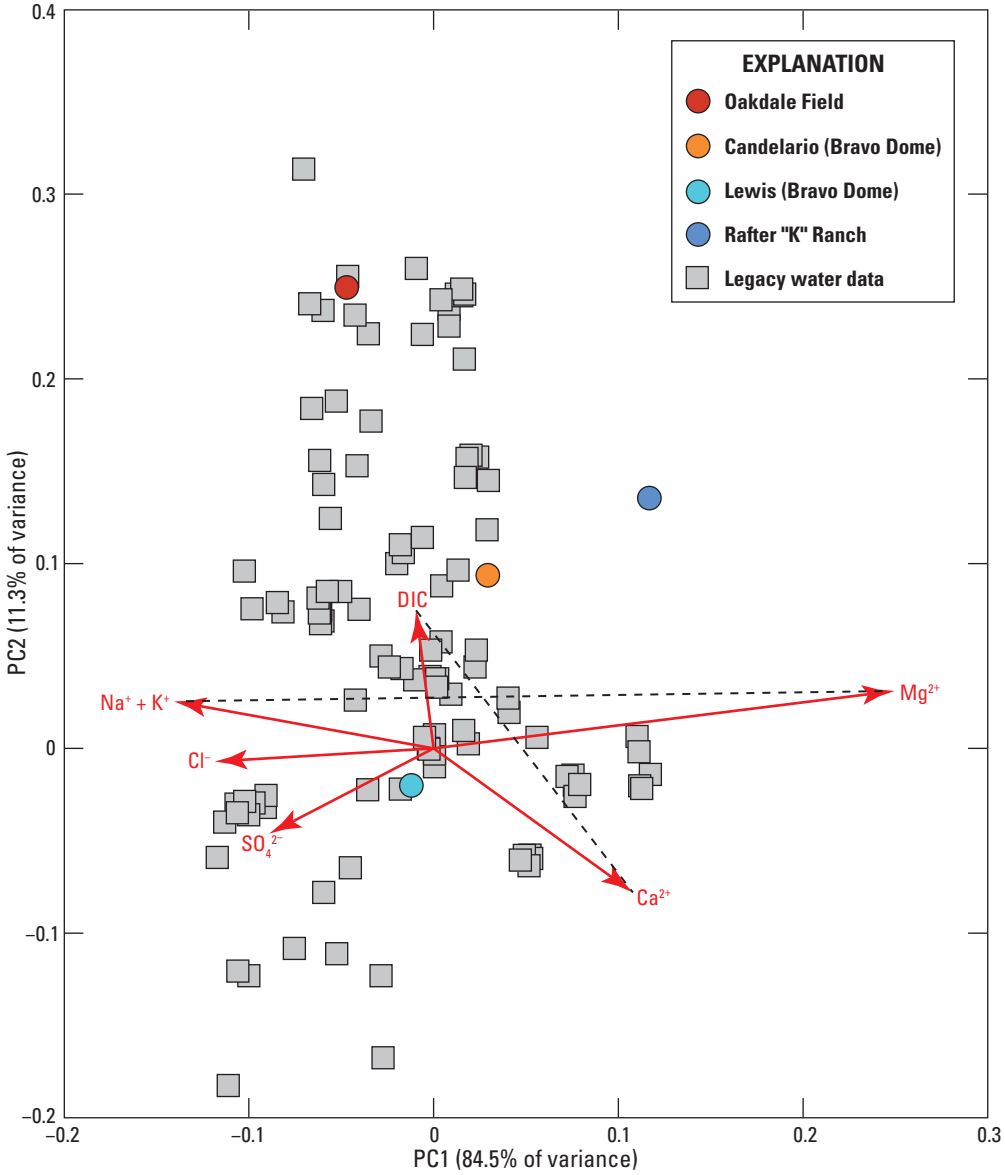

Figure 2. Compositional biplot that represents a principle component (PC) analysis of centered log ratio (clr)-transformed water-chemistry data for produced water samples and legacy data. PC1 explains 84.5 percent (%) of the variance in the dataset, and PC2 explains 11.3 percent of the variance. The dashed lines represent examples of links between the rays. Ca^{2+}, calcium; Cl^{-}, chloride; DIC, dissolved organic carbon; K^{+}, potassium; Mg^{2+}, magnesium; Na^{+}, sodium; SO_4^{2-}, sulfate.

with oxygen-18 in the water, causing the $\delta^{18}O\text{-}H_2O$ value to decrease over time; however, isotopic equilibrium is quickly achieved, and this fractionation is rarely observed in nature (Clark and Fritz, 1997). Exchange with CO_2 would not cause the deviation observed in the dataset. These samples may also be influenced by microbial activity (for example, microbial methanogenesis; Balabane and others, 1987; Whiticar, 1999) and mixing of water sources. Moreover, the isotopic composition of these waters may simply reflect the isotopic values during recharge and could be slightly influenced by mixing with basinal brines (Clayton and others, 1966). Because this study does not have known mixing endmembers for either water isotope, establishing mixing trends is difficult.

The $^{87}Sr/^{86}Sr$ isotopic system is typically used to determine mixing of groundwaters or used as a tracer for sources of salinity or water-rock interactions (Geyh and others, 2001).

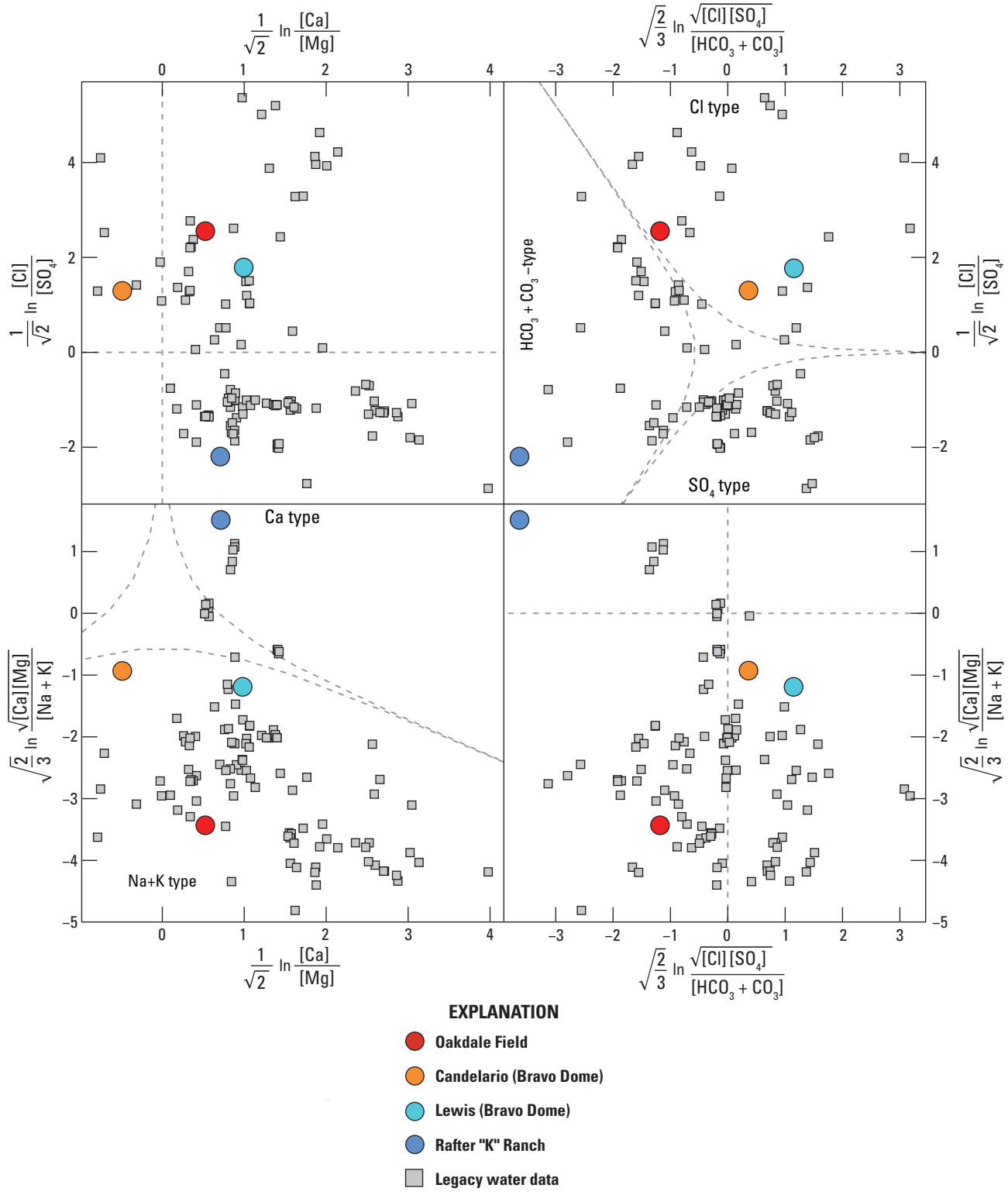

Figure 3. Isometric log-ratio ion plot (as described in Shelton, Engle, and others, 2018) showing the major ion composition of produced water samples and legacy data. Square brackets indicate concentration in milliequivalents per kilogram. Ca, calcium; Cl, chloride; CO_3, carbonate; HCO_3, bicarbonate; K, potassium; ln, natural logarithm; Mg, magnesium; Na, sodium; SO_4, sulfate. Gray dashed lines indicate which species dominates in each quadrant, as labeled.

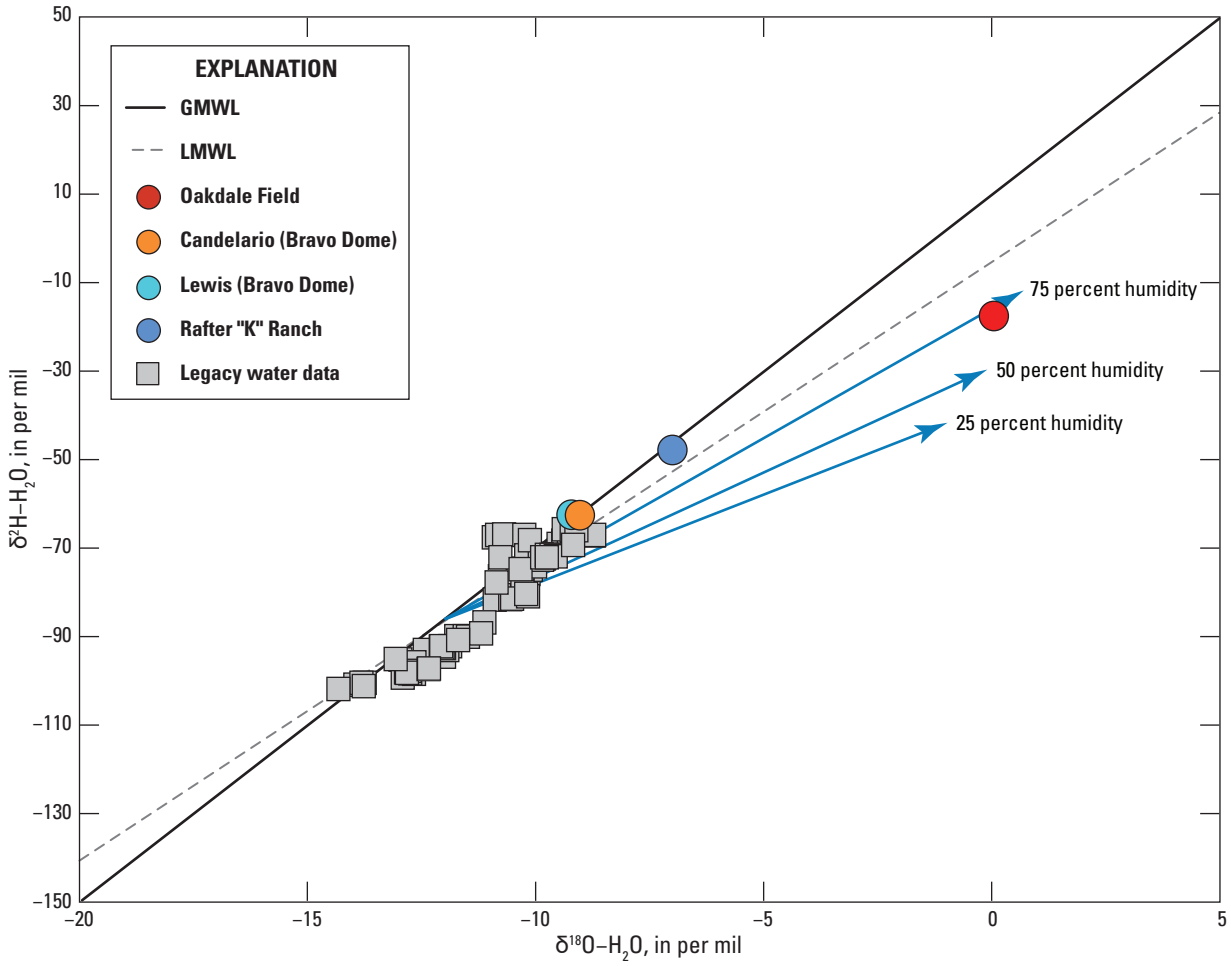

Figure 4. Graph showing water isotope data for produced water samples and legacy data relative to the global meteoric water line (GMWL) and a local meteoric water line (LMWL; developed for U.S. Geological Survey station number 08382650; Coplen and Kendall, 2000). Humidity trajectories were calculated using 25, 50, and 75 percent humidity (solid blue lines), a temperature of 25 degrees Celsius, and fractionation factors for water-vapor exchange for oxygen-18 and deuterium from Kakiuchi and Matsuo (1979). δ^2H-H_2O and $\delta^{18}O$-H_2O are measured relative to Vienna Standard Mean Ocean Water (VSMOW).

The two Bravo Dome samples, Lewis and Candelario, have more radiogenic strontium (Sr) than the Rafter "K" Ranch and Oakdale Field waters, meaning that the Lewis and Candelario $^{87}Sr/^{86}Sr$ values are greater than the Rafter "K" Ranch and Oakdale Field $^{87}Sr/^{86}Sr$ values (fig. 5). The Oakdale Field sample is the only sample that conforms to the general regional trend for Sr isotopes and concentrations; the Rafter "K" Ranch sample has a much lower Sr concentration than the other samples, and the Bravo Dome samples are much more radiogenic than the legacy water samples. The legacy water data, which are time-series data from multiple surface-water sites, monitoring wells, domestic water wells, and production wells, show little variation between time points, only small changes in the Sr concentrations in the sampled water (the $^{87}Sr/^{86}Sr$ values for the same locations at different time points remain more constant). All of the water data, including the four samples collected for the current study and the legacy data, are within the isotopic range of the data for the regional rocks, which are volcanic, xenolithic, plutonic, or unknown rock types. The hard rock data are much more variable than the legacy water data, with $^{87}Sr/^{86}Sr$ values ranging from 0.70274 to 0.80837 and 1/Sr values ranging from 0.00029 kilogram per milligram (kg/mg) to 192.3 kg/mg (EarthChem, 2018).

The Lewis and Candelario samples (from the West Bravo Dome exploration unit) and the Oakdale Field sample generally align with overall regional geochemical trends, except for the few differences outlined above: the Oakdale Field sample is isotopically enriched in oxygen-18 and deuterium (^2H) compared to the legacy water data, and the Bravo Dome samples (Lewis and Candelario) have greater $^{87}Sr/^{86}Sr$ values compared to the legacy water data. The Rafter "K" Ranch sample appears to be an outlier, as it generally deviates from regional water trends outlined by the legacy water data (see figs. 2–4). The greater amounts of radiogenic strontium in the

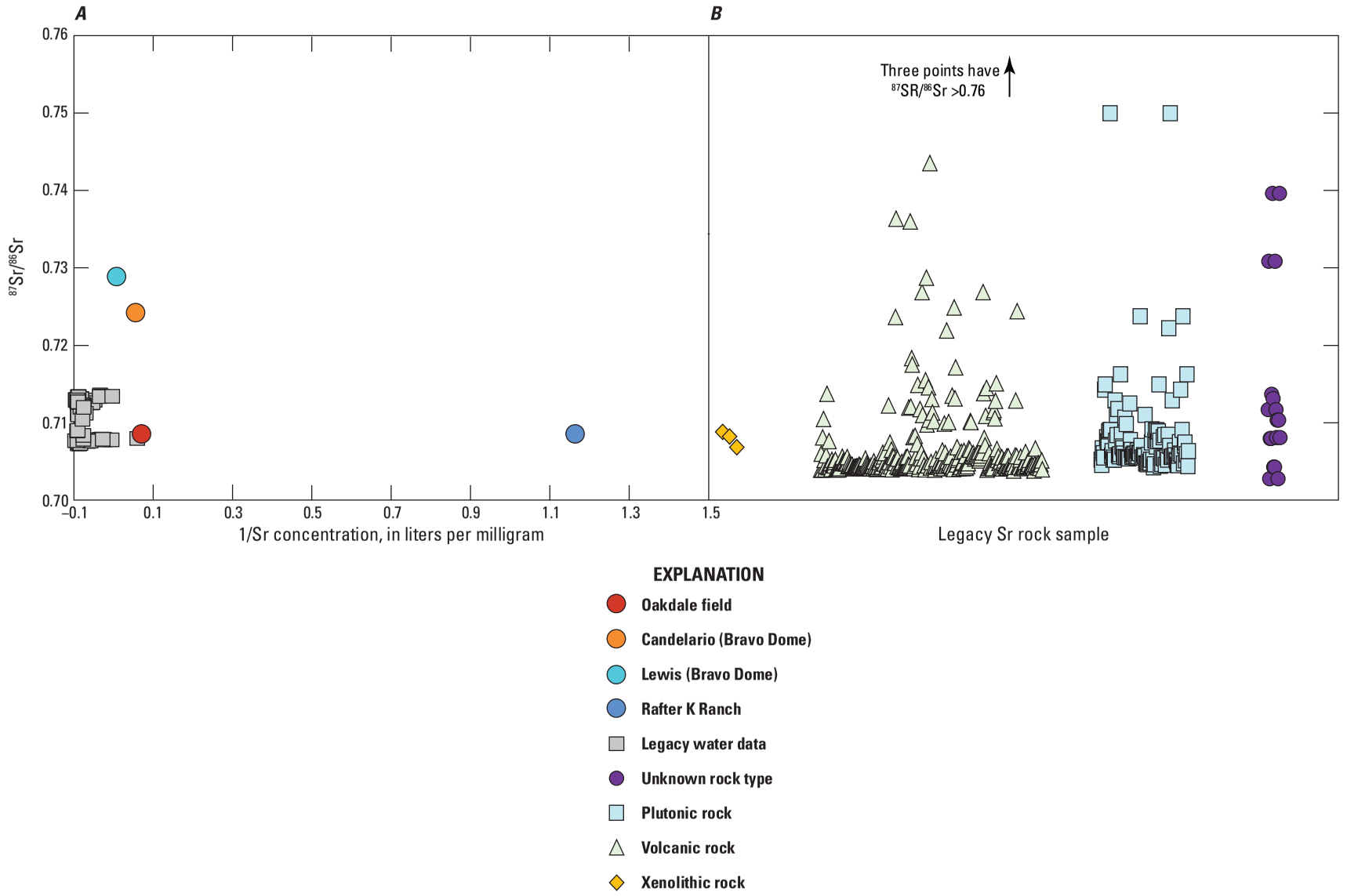

Figure 5. *A*, Graph showing strontium (Sr) concentrations and isotope ratios (strontium-87/strontium-86 [$^{87}Sr/^{86}Sr$]) for the four produced water samples and legacy water data. The x-axis has been scaled to better display the four samples from the current study. *B*, Graph showing Sr isotope ratios for the legacy rock data. Three of the points are outside the range of the y-axis, in the direction indicated by the black arrow (values are 0.768, 0.808, and 0.808). No data are plotted on the x-axis in *B*.

Lewis and Candelario samples cannot be explained by the high CO_2 content of the reservoir and is more likely explained by volcanism in the localized area. Previous volcanic activity occurred near Bravo Dome, specifically in the Raton Volcanic Field (Broadhead and others, 2009). Sathaye and others (2014) hypothesized that the CO_2 gas that charged Bravo Dome was likely sourced from the formation of the Capulin Volcano in the Raton Volcanic Field and traveled into the basin via faults generated by magmatic activity. It is also possible that the high CO_2 content (that is, acidity) of these waters may be dissolving formation rock, thus releasing radiogenic strontium. The similarity of the strontium isotope values and concentrations of the Lewis and Candelario samples may indicate a common source for the groundwater, similar residence times, and (or) similar flow paths.

The Oakdale Field sample is most different from the legacy water data in terms of isotopic composition. The Oakdale Field water has much more positive δ^2H and $\delta^{18}O$ values (fig. 4). The Oakdale Field sample could have been affected by evaporation during recharge, which is a process that can increase both the δ^2H and $\delta^{18}O$ values in water, causing the sampled water to have larger δ^2H and $\delta^{18}O$ values than the GMWL (for example, Clark and Fritz, 1997). These high δ^2H and $\delta^{18}O$ values could imply different recharge areas or time of recharge than the other samples examined in this study. Also, because the Oakdale Field sample was collected from an open storage tank, water may have evaporated from the storage tank itself, altering the isotopic composition of the water post-production. The tank was not well mixed, however, and the sample was collected from the bottom of the tank, which might have deterred major evaporative and depositional effects. Microbial activity may also affect the isotopes of produced water, such as $\delta^{18}O$-H_2O; Oakdale Field may be actively methanogenic because of the CH_4 produced from the field (Worrall, 2004).

The Rafter "K" Ranch sample is the most geochemically distinct of the four samples collected in the current study, differing both isotopically and compositionally. This deviation from regional trends may be due to the shallow sampling depth. Much of the legacy data, however, are from regional surface and monitoring wells, which would also reflect shallow conditions. The difference in depth between Rafter "K" Ranch and the other three CO_2-rich samples collected in this study may explain some of the differences observed between those two groups of samples. The Bravo Dome (Lewis and Candelario) and Oakdale Field samples are all Na^++K^+- and Cl^--type waters, typical of basinal brines (Kharaka and Hanor, 2003), whereas Rafter "K" Ranch is Ca^{2+}- and HCO_3^-+CO_3^{2-}-type water, typical of low-salinity, shallow groundwaters. This observation is consistent with the much lower TDS value of the Rafter "K" Ranch sample compared to the other three sites (see table 2). The shallow groundwater samples from the legacy water data are also typically dominated by SO_4^{2-}, with some samples being HCO_3^-+CO_3^{2-} type, and are either Ca^{2+} type or do not have a dominant cation (fig. 3).

Two differences between the shallow legacy groundwater samples and the Rafter "K" Ranch sample are CO_2 concentration and producing strata. The CO_2 concentration of the Rafter "K" Ranch sample is much higher than those of the legacy data, as the legacy data are not from either naturally producing CO_2 wells or gas wells. This difference most likely explains the dominance in DIC for Rafter "K" Ranch compared to SO_4^{2-} for most of the shallow legacy groundwater samples because CO_2 injection into shallow groundwaters increases the alkalinity as the CO_2 dissolves into formation water (for example, Kharaka and others, 2010; Peter and others, 2012). Unfortunately, the exact lithological effects are uncertain because the producing strata for the legacy water data are unknown and the producing strata for Rafter "K" Ranch are uncertain.

Despite the possible effects of CO_2 described above, and even though all four samples have different geochemical signatures, the samples generally fit regional geochemical trends associated with producing wells across southern Colorado and northeastern New Mexico. Regional dissimilarities between the two Bravo Dome samples and the legacy data may be due to different flow paths, causing differing water-rock interactions (specifically, accumulation of radiogenic strontium). The Oakdale Field sample generally conforms to regional trends, except for the isotopic values of the formation water ($\delta^{18}O$ and δ^2H of H_2O). This deviation may be due to different recharge times, evaporation during recharge, evaporation in the storage tank, and (or) microbial activity. The Rafter "K" Ranch sample appears to be the most distinct when comparing geochemistry to the legacy data; the sample has much less strontium, more enriched $\delta^{18}O$ and δ^2H values for H_2O, and is Ca-HCO_3-type water. Some of these deviations can easily be attributed to the well's shallow sampling depth and higher CO_2 concentration compared to other shallow groundwaters included in the legacy data. Because some of the legacy data are from surface waters and shallow groundwater wells, it appears that depth alone is not driving the differences observed. Differences may be driven by lithology because the Rafter "K" Ranch producing formation is like that of Bravo Dome, which produces from much greater depths than the shallow legacy samples.

Microbial Community Composition and Diversity

To better understand how high-CO_2 environments affect the microbial communities in produced water, the microbial community compositions of the four collected samples were analyzed. The average number of sequences per sample prior to rarefaction was 38,488, with the minimum and maximum number of sequences equal to 26,762 and 64,702, respectively (table 3). Samples were rarefied by random subsampling to 24,000 sequences per sample for community analysis. After rarefaction, the average number of OTUs identified in each sample was 141, with Candelario having

the most OTUs identified (252 OTUs) and Lewis having the fewest (41 OTUs). The microbes identified in these four samples span 28 phyla and 480 OTUs, with OTUs from only 5 of the 28 phyla present in each sample (Actinobacteria, Bacteroidetes, Euryarchaeota, Firmicutes, and Proteobacteria). Most OTUs identified (84.0 percent) were found in only one of the four samples collected, and only one OTU was identified in all four samples. Rafter "K" Ranch, the shallowest groundwater sample and the hydrogeochemical outlier, had the highest Shannon diversity index (Shannon, 1948), 3.94. The Lewis sample (collected from the West Bravo Dome Unit) had the lowest Shannon diversity index, 1.80. Bacteria dominated all samples, with Archaea present in the four water samples at a percent abundance between 0.0 and 0.3 percent (table 3). On average, the most prominent phyla in the four water samples were Firmicutes (30.5 percent), Proteobacteria (28.8 percent), Bacteroidetes (26.8 percent), and Chloroflexi (5.0 percent).

The most prominent genera identified in the four water samples, on average, were *Acetobacterium* (8.0 percent), *Desulfovibrio* (5.7 percent; the only genus present in all four water samples), *Pseudomonas* (4.9 percent), *Sphingobacterium* (4.7 percent), and *Sulfurospirillum* (4.3 percent). The Lewis well sample is dominated by unclassified Bacteroidetes (50.8 percent), *Desulfotomaculum arcticum* (12.0 percent), and *Meniscus* sp. (10.5 percent). The genus *Meniscus* is understudied; however, the few existing studies have suggested that the genus is aerotolerant and heterotrophic (Irgens, 1977). *Desulfotomaculum arcticum* is a relatively thermophilic SRB isolated from sediment (Vandieken and others, 2006); other species of the *Desulfotomaculum* genus were identified in an aquifer used for natural gas storage (Berlendis and others, 2016). Some species of the genus *Desulfotomaculum* can oxidize organic compounds to CO_2, whereas other species use CO_2 and H_2 to grow autotrophically (Kuever and Rainey, 2015). Therefore, some of the CO_2 co-produced at the Lewis well could have been microbially modified, either added or removed from the system by the in situ organisms. Bacteroidetes is a very diverse phylum, with species identified in various environments, such as soils, the guts of humans and animals, sludge, and biodegraded oil reservoirs (for example, Grabowski and others, 2005; Weon and others, 2006; De Filippo and others, 2010; Sun and others, 2016; Sierra-Garcia and others, 2017).

The water produced from the Candelario well is dominated by *Sphingobacterium faecium* (16.9 percent), *Pseudomonas* sp. (15.2 percent), and unclassified organisms (10.6 percent). Little is known about *S. faecium* other than that they are aerobic and "of feces"; however, species of the genus *Sphingobacterium* have been identified in soils, compost, and industrial applications and are known etiological agents of infection (Takeuchi and Yokota, 1992; Lambiase, 2014). Species of the genus *Pseudomonas* have been identified in many different habitats and have been isolated from environments including human clinical specimens, soils, marshes, and marine environments (for example, Hardalo and Edberg, 1997; Stover and others, 2000; Palleroni, 2015).

The difference in microbial communities between the two Bravo Dome sites (Lewis and Candelario) combined with dissimilar hydrogeochemistry and similar producing strata may support the hypothesis that the Bravo Dome hydrologic system is compartmentalized. If the two wells were hydrologically connected, they would be expected to be more microbiologically and geochemically similar. Due to the difference in well depth (approximately 90 m), however, differences in pressure and water residence time could also be driving these general microbial and geochemical differences.

The Oakdale Field sample contained mostly *Acetobacterium* sp. (31.7 percent), *Desulfovibrio dechloracetivorans* (18.0 percent), *Sulfurospirillum* sp. (16.0 percent), uncultured *Marinobacterium* sp. (14.3 percent), and Campylobacteraceae (11.6 percent). Species of the genus *Acetobacterium* are diverse in their functions and habitats (Stackebrandt, 2014) and are categorized as CO_2-reducing, hydrogen-oxidizing anaerobes (Balch and others, 1977). *Desulfovibrio dechloracetivorans* is a dechlorinating SRB that has been isolated from marine and tidal mudflat sediment, as well as from crude oil facilities (Sun and others, 2000). Species of the genus *Sulfurospirillum* are free-living bacteria

Table 3. Results of 16S ribosomal ribonucleic acid (rRNA) gene amplicon sequencing.

[The total number of sequences is the number identified after singleton removal. Diversity statistics and percent Bacteria and Archaea were determined after removal of singletons and contaminants and rarefaction to 24,000 sequences per sample. OTU, operational taxonomic unit]

Sample	Total sequences per sample	Species richness	Shannon diversity index	Pielou's evenness	Percent Bacteria	Percent Archaea	Most abundant OTU (percent abundance)
Lewis (Bravo Dome)	27,743	41	1.80	0.484	100	0	Unknown Bacteroidetes (50.8)
Candelario (Bravo Dome)	26,762	252	3.75	0.679	99.7	0.3	*Sphingobacterium feacium* (16.9)
Oakdale Field	34,743	70	1.96	0.462	100	0	*Acetobacterium* spp. (31.7)
Rafter "K" Ranch	64,702	199	3.94	0.744	99.8	0.2	Uncultured Blvii28 wastewater-sludge group (9.3)

that have been isolated from water produced from an oil field (Hubert and Voordouw, 2007), as well as anaerobic sludge, surface water, and anoxic muds (Lastovica and others, 2014). The genus *Marinobacterium* contains species that have been identified in mostly marine environments, including pulp mill effluent water, tidal flats, and marine sediment (González and others, 1997). Genera of the family Campylobacteraceae are very diverse, have a wide range of growth characteristics, and tend to be identified in humans, animals, surface water, and groundwater (Lastovica and others, 2014).

The Rafter "K" Ranch sample is dominated by the Blvii28 wastewater-sludge group (9.3 percent), *Leptolinea* sp. (7.3 percent), and uncultured Veillonellaceae (6.5 percent). The Blvii28 wastewater-sludge group is a poorly characterized group of organisms commonly identified in sewage-sludge digesters or anaerobic wastewater that have yet to be isolated (Su and others, 2014). Species of the genera *Leptolinea* are strict mesophilic anaerobes and have been isolated from an artificial wastewater-sludge digestor (Yamada and others, 2006). Genera of the family Veillonellaceae are identified in the microbiomes of many animals and humans (Marchandin and Jumas-Bilak, 2014). Because all three of these bacteria types are frequently associated with human or animal waste, it appears that water infiltrating into the shallow, likely unconfined aquifer is carrying surficial animal waste products into the subsurface during recharge. Ranching in the surrounding areas, mostly cattle and horses, could contribute to the microbiological signature observed in this shallow groundwater well. Furthermore, because the well could not be adequately purged prior to sample collection (see the "Methods" section), the microbes may have been concentrated near the wellbore.

A nonmetric multidimensional scaling (NMDS) plot using a UniFrac distance matrix shows that the four water samples plot separately from each other, indicating some differences in sample composition at the OTU level (fig. 6*A*). Notably, the Oakdale Field sample was the most distinct of the four, and this difference was confirmed by using permutated analysis of variance with the adonis2 function in the vegan package of R (Oksanen and others, 2013), resulting in a R^2 value of 1 and a *p*-value of 0.25 (fig. 6*A*). This result may be due to either the mixture of waters creating the Oakdale Field sample or the open-air tank possibly causing changes in the microbial community post-production. Multilevel pattern analysis (multipatt function in the indicspecies package of R; De Cáceres and Legendre, 2009) was used on five groups and did not identify any indicator species. The groups analyzed were (1) Candelario versus the remaining three water samples, (2) Lewis versus the remaining three water samples, (3) Oakdale Field versus the remaining three water samples, (4) Rafter "K" Ranch versus the remaining three water samples, and (5) the two Bravo Dome samples (Lewis and Candelario) versus the Rafter "K" Ranch and Oakdale Field water samples.

Data from Freedman and others (2017) were added to the analysis to compare McElmo Dome, a commercial CO_2 reservoir in Colorado, to Bravo Dome (fig. 6*B*). McElmo Dome produces CO_2 at a comparable quality (approximately 99 percent CO_2 by composition) to Bravo Dome (Shelton and others, 2016; Freedman and others, 2017). The six samples—two from Bravo Dome, two from McElmo Dome well 3, and two from McElmo Dome well 10—were dissimilar, the only clustering being the two points for each McElmo Dome well. An adonis2 analysis between the four McElmo Dome samples (group 1) and the two Bravo Dome samples (group 2) yielded an R^2 value of 0.40 and a *p*-value of 0.067, indicating that the differences across the groups are greater than the differences within the groups.

The significance of relations between any hydrologic or gas phase parameters (for example, Na^+, SO_4^{2-}) and microbial community structure was tested with the envfit function in the R package vegan. No hydrologic data were significantly associated with the UniFrac-based ordination; *p*-values ranged from 0.1250 (sodium) to 1.0000 (magnesium). Furthermore, the associated gas composition data collected by Brennan (2017) were used to determine if the CO_2 concentration (or any other identified gas) had any significant linkage to differences in microbial community structure. No significant results were obtained; the *p*-value for CO_2 concentration was 0.4806, and *p*-values for helium (He), argon (Ar), N_2, CH_4, and hydrocarbons measured in the gas with greater than or equal to two carbon atoms (C_{2+}) concentrations were all greater than 0.5. These results indicate that neither gas composition nor water chemistry have any significant effect on the differences between the microbial communities of the four water samples collected for the current study.

This result is particularly interesting considering that the Oakdale Field sample, when compared to the three other water samples, is associated with an analysis of similarities R value of 1 and a *p*-value of 0.25. The Oakdale Field water sample is a composite of water from wells producing water and gas with varying concentrations of CO_2 and was the only sample that was not associated with gas at greater than 99 percent CO_2. It was also the only sample of the four that had co-produced hydrocarbons and biogenic gas. Given that the CO_2 concentration was not a statistically significant driver of the microbial differences observed between the four samples, differences in CO_2 concentrations are not driving the observed differences in microbial community structure.

These results differ from the findings of Ham and others (2017), who observed significant variation between microbial communities in two sites with high CO_2 concentrations. They observed that some geochemical factors were significantly associated with the microbial communities—total dissolved solids, alkalinity, pH, strontium, lithium, cesium, and CH_4—and CO_2 concentrations were also linked to the microbial data (Ham and others, 2017). Their results suggest that CO_2 concentrations, as well as some geochemical factors, may drive the observed microbial community differences in CO_2-rich aquifers. The authors stated, however, that oxidation-reduction (redox) conditions in the subsurface aqueous environment may be more of a driving factor for microbial community diversity than CO_2 concentrations, which may be applicable

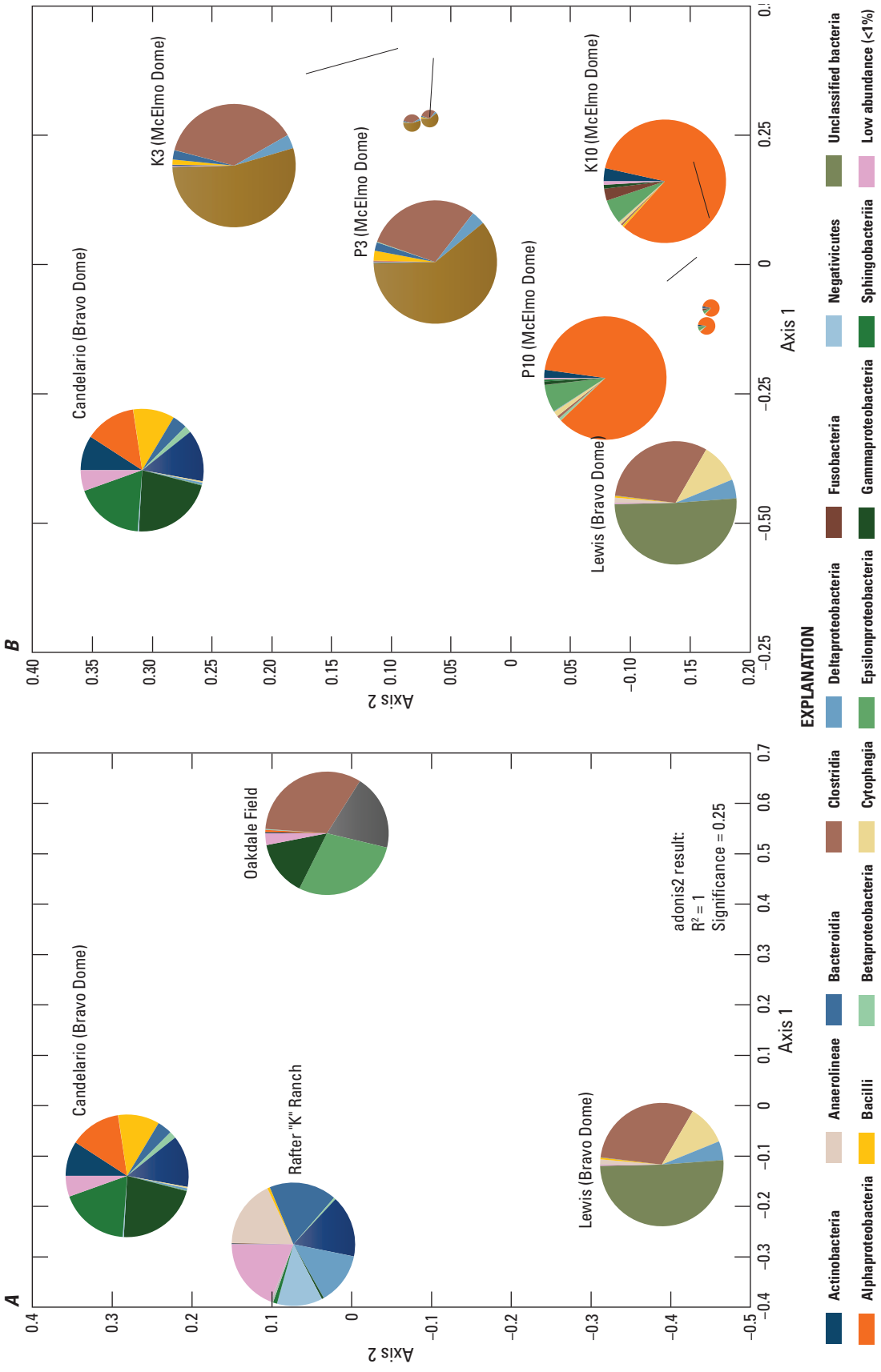

Figure 6. Nonmetric multidimensional scaling (NMDS) plots based on UniFrac distance matrices, with point locations represented by pie charts showing microbiology of the water samples at the class level. All classes listed were observed at an abundance of at least 1 percent (%); all classes identified at less than 1 percent were grouped together. *A*, NMDS plot for the four samples collected in the current study; the adonis2 result shown is for Oakdale Field versus the remaining three samples. *B*, NMDS plot for the two Bravo Dome samples collected for the current study and four samples collected from McElmo Dome in southwestern Colorado (Freedman and others, 2017). The McElmo Dome data are for two samples collected from two wells.

in the current study. These differences between the current study and the study by Ham and others (2017) may be due to differences in DNA extraction methods, as observed by others (Cruaud and others, 2014; Mazziotti and others, 2018), or may be because the current study is more diverse in that the four samples analyzed were taken from three different subsurface environments.

Growth and Activity of Microbial Functional Groups in the Rafter "K" Ranch and Oakdale Field Samples

To assess the potential activity of microorganisms in a CO_2 sequestration analogue, six microbial functional groups were targeted by using anaerobic cultivation in selective media under elevated CO_2 headspace and varying salinities. Six microbial functional groups (autotrophs, FeRB, methanogens, NRB, SRB, and heterotrophs) were successfully cultured from both the Rafter "K" Ranch and Oakdale Field water samples (table 4). Water was not collected from the two Bravo Dome sites for anaerobic cultivation. The most growth and activity were observed in cultures with media salinities approximating that of the produced waters: 1 g/L NaCl for Rafter "K" Ranch and 20 g/L NaCl for Oakdale Field. No growth was observed in any of the cultivation controls (no inoculum).

Heterotroph and NRB cultures grew to the highest densities, as indicated by visual observations, which is not surprising because they were provided high concentrations of easily metabolized carbon substrates (peptone yeast extract glucose and glycerol, respectively). Growth was observed more quickly for heterotrophs compared to NRB cultures from the same media salinity, CO_2 level, and site. Despite the ample growth and high level of biomass observed, nitrate

Table 4. Growth and activity for microbial functional groups enriched from the Rafter "K" Ranch and Oakdale Field water samples under 20 or 100 percent carbon dioxide (CO_2) headspace.

[Growth was assessed visually by changes in turbidity, with growth ranging from low (+) to high (++++) turbidity or no growth (−). The activity of iron-reducing bacteria (FeRB) was confirmed by measuring accumulation of divalent iron, Fe(II). The activity of heterotrophs, autotrophs and methanogens was confirmed by measuring accumulation of methane (CH_4). Decreasing nitrate (NO_3^-) concentration confirmed the activity of nitrate-reducing bacteria (NRB). For sulfate-reducing bacteria (SRB), the presence (+) or absence (−) of hydrogen sulfide (H_2S) was used to confirm activity. The intensity of H_2S production was based on color change of lead acetate strips when in contact with a droplet of culture medium (none, no color change; +, faint color change; ++, moderately strong color change; and +++, intense color change). g/L, gram per liter; mmol/L, millimole per liter; µmol/L, micromole per liter; NaCl, sodium chloride; ND, none detected; BDL, below detection limit]

Inputs			Outputs					
Inoculum source	Percent headspace CO_2	Media salinity (g/L NaCl)	FeRB growth/ Fe(II) (mmol/L)	SRB growth/ H_2S	NRB growth/ NO_3^- (mmol/L)	Heterotrophs growth/CH_4 (µmol/L)	Autotrophs growth/CH_4 (µmol/L)	Acetoclastic methanogens growth/CH_4 (µmol/L)
Oakdale Field	20	1	+++/25.84	+/++	+/33.00	+++/2.05	+/5.33	+/0.96
	100	1	+++/17.00	+/++	+++/28.42	++/0.01	+/7.34	+/0.61
	20	20	+++/19.21	++/+++	++/11.32	++++/24.34	++/9.59	+/0.01
	100	20	+++/18.61	+++/++	+++/22.42	+++/2.65	++/8.90	+/0.81
	20	100	weak +/2.23	weak +/none	+/38.10	++/0.01	−/ND	−/0.02
	100	100	+/1.42	−/none	−/40.25	++/0.01	−/ND	−/0.01
Rafter "K" Ranch	20	1	++/7.65	++/++	+++/0.04	++/0.31	++/11.75	−/0.01
	100	1	++/8.46	++/++	+/40.14	+/0.07	++/7.94	−/BDL
	20	20	−/1.02	+/+	+/30.39	+++/0.06	−/ND	−/BDL
	100	20	−/0.92	−/none	++/38.92	+++/0.04	weak +/0.09	−/BDL
	20	100	−/0.97	−/none	++/33.87	−/0.23	−/ND	−/0.01
	100	100	−/0.97	−/none	−/39.32	+/0.20	−/ND	−/BDL
Control	20	1	−/1.07	−/none	−/40.90	−/0.01	−/ND	−/BDL
	100	1	−/1.12	−/none	−/38.92	−/0.01	−/ND	−/0.01
	20	20	−/1.07	−/none	−/40.88	−/0.01	−/ND	−/BDL
	100	20	−/1.12	−/none	−/41.75	−/0.01	−/ND	−/0.01
	20	100	−/0.92	−/none	−/37.83	−/BDL	−/ND	−/BDL
	100	100	−/0.82	−/none	−/41.99	−/BDL	−/ND	−/BDL

was reduced in only a subset of the NRB cultures (table 4). This result indicates that most organisms enriched in NRB cultures were growing fermentatively and were not using the supplemental nitrate as a terminal electron acceptor. Taken together, these observations suggest that influxes of organic carbon to either the Oakdale Field or Rafter "K" Ranch groundwater could stimulate rapid microbial growth. The high biomass resulting from the addition of organic-rich, fermentable substrates could lead to biofouling during in situ CO_2 injection activities.

Methane production was observed under heterotrophic, autotrophic, and methanogenic culture conditions (table 4). Autotrophic cultures, which were supplied H_2 as electron donor, were the most consistent producers of CH_4, followed by heterotrophic cultures from Oakdale Field, heterotrophic cultures from Rafter "K" Ranch, and methanogenic cultures from Oakdale Field. No growth was observed under methanogenic conditions for cultures from Rafter "K" Ranch, and the growth and activity under methanogenic conditions for cultures from Oakdale Field were among the lowest of all cultures across treatments, suggesting that either the acetate supplied as electron donor and (or) the methanogenic culture media were not metabolically favored by the microbiota of either site. Hydrogenotrophic methanogenesis ($CO_2 + 4H_2 \rightarrow CH_4 + 2H_2O$) was likely the source of all or most observed CH_4, with H_2 provided in autotrophic cultures or generated through organic carbon degradation in the other cultures. The organic carbon substrates provided (for example, citrate, lactate, glucose, and glycerol) can be degraded via fermentation, resulting in the production of H_2 (Madigan and others, 2012), which can be used by hydrogenotrophic methanogens. The viability of methanogens in the Rafter "K" Ranch and Oakdale Field samples indicates that these populations have the potential to generate CH_4 in situ if a hydrogen source is available.

Significant iron and SO_4^{2-} concentrations were found in waters from both Rafter "K" Ranch and Oakdale Field (table 2), so it is reasonable to suspect that anaerobic cycling of both iron and sulfur occur in these groundwaters. Although anaerobic oxidation of these elements was not tested, activity of FeRB and SRB was confirmed by production of Fe(II) and H_2S as end-products of trivalent iron (Fe[III]) and SO_4^{2-} reduction, respectively (table 4). Our results indicate that Oakdale Field FeRB and SRB are versatile; they were able to grow over a range of salinities and CO_2 levels, but FeOOH appeared to be a more favorable electron acceptor than SO_4^{2-}. In contrast, Rafter "K" Ranch FeRB and SRB grew only at the 1-g/L-NaCl salinity, with only modest growth and activity, and neither electron acceptor seemed to be favored. Thus, there is potential for well souring via microbial SO_4^{2-} reduction at both sites under the in situ conditions. Fluctuations in salinity at Rafter "K" Ranch, however, could inhibit microbial iron and SO_4^{2-} reduction (as well as microbial growth in general), whereas Oakdale Field microbes may show little response to any (at least modest) change in salinity.

Conclusions

Studies of natural CO_2 in reservoirs have the potential to offer insight into the effects of geologic CO_2 sequestration. Here, samples from four naturally occurring CO_2 reservoirs were analyzed to determine how these CO_2-rich habitats affected the regional hydrology and microbial ecology of the subsurface. Although the sample size was small (n=4) and some sampling conditions were not ideal (for example, few sample sites were available from the Bravo Dome commercial unit), the hydrogeochemistry of the two Bravo Dome samples generally aligned with regional hydrogeochemical trends. The two Bravo Dome samples were geochemically different from each other, possibly suggesting compartmentalization in the reservoir, as suggested by previous studies. The Oakdale Field sample was isotopically different from regional trends, and the Rafter "K" Ranch sample was dramatically different from regional legacy water data, possibly due to high DIC concentrations induced by the high CO_2 content in the well.

Although the microbial community composition of the Oakdale Field sample differed from the other samples, the microbial ecology of the four wells could not be tied to any hydrogeochemical or gas geochemical parameters, nor were any OTUs significantly associated with a site. Differences in microbial ecology across the four sites may be linked to redox conditions or differences in lithology. Although no hydrogeochemical parameters were significantly associated with the microbial ecology of the samples, they still may be influencing the microbial community composition to some extent.

Distinct patterns in microbial growth and activity by site underscore the importance of local groundwater geochemistry and microbial ecology in predicting the outcomes of CO_2 injection into deep geologic formations. Moreover, the strong stimulatory effects of nutrient amendments, particularly bioavailable carbon, on the elevated CO_2-tolerant microbes show that unintended influxes into the subsurface systems, such as septic tank leakage, can greatly alter microbial responses. Taken together, these observations suggest that natural biogeochemical conditions and regional anthropogenic activities must be accounted for in the long-term planning of a CO_2 injection project.

References Cited

Aitchison, J., 1986, The statistical analysis of compositional data: London, Chapman & Hall, 416 p.

Akhbari, D., and Hesse, M.A., 2017, Causes of underpressure in natural CO_2 reservoirs and implications for geological storage: Geology, v. 45, no. 1, p. 47–50, accessed January 2018 at https://doi.org/10.1130/G38362.1.

Allis, R., Chidsey, T., Gwynn, W., Morgan, C., White, S., Adams, M., and Moore, J., 2001, Natural CO_2 reservoirs on the Colorado Plateau and southern Rocky Mountains—Candidates for CO_2 sequestration, *in* Proceedings of the First National Conference on Carbon Sequestration, Washington, D.C., May 14–17, 2001: Morgantown, W.Va., U.S. Department of Energy, National Energy Technology Laboratory, 19 p.

Apprill, A., McNally, S., Parsons, R., and Weber, L., 2015, Minor revision to V4 region SSU rRNA 806R gene primer greatly increases detection of SAR11 bacterioplankton: Aquatic Microbial Ecology, v. 75, no. 2, p. 129–137. [Also available at https://doi.org/10.3354/ame01753.]

Baines, S.J., and Worden, R.H., 2004, Geological storage of carbon dioxide, *in* Baines, S.J., and Worden, R.H., eds., Geological storage of carbon dioxide: London, Geological Society of London Special Publication, v. 233, p. 1–6, accessed January 2018 at https://doi.org/10.1144/GSL.SP.2004.233.01.01.

Balabane, M., Galimov, E., Hermann, M., and Létolle, R., 1987, Hydrogen and carbon isotope fractionation during experimental production of bacterial methane: Organic Geochemistry, v. 11, no. 2, p. 115–119, accessed January 2018 at https://doi.org/10.1016/0146-6380(87)90033-7.

Balch, W.E., Schoberth, S., Tanner, R.S., and Wolfe, R.S., 1977, *Acetobacterium*, a new genus of hydrogen-oxidizing, carbon dioxide-reducing, anaerobic bacteria: International Journal of Systematic and Evolutionary Microbiology, v. 27, no. 4, p. 355–361, accessed January 2018 at https://doi.org/10.1099/00207713-27-4-355.

Ballentine, C.J., Schoell, M., Coleman, D., and Cain, B.A., 2001, 300-Myr-old magmatic CO_2 in natural gas reservoirs of the west Texas Permian Basin: Nature, v. 409, p. 327–331. [Also available at https://doi.org/10.1038/35053046.]

Baltz, E.H., 1965, Stratigraphy and history of Raton Basin and notes on San Luis Basin, Colorado-New Mexico: American Association of Petroleum Geologists Bulletin, v. 49, p. 2041–2075, accessed January 2018 at https://doi.org/10.1306/A6633882-16C0-11D7-8645000102C1865D.

Barberán, A., Ladau, J., Leff, J.W., Pollard, K.S., Menninger, H.L., Dunn, R.R., and Fierer, N., 2015, Continental-scale distributions of dust-associated bacteria and fungi: Proceedings of the National Academy of Sciences of the United States of America, v. 112, no. 18, p. 5756–5761, accessed January 2018 at https://doi.org/10.1073/pnas.1420815112.

Berlendis, S., Ranchou-Peyruse, M., Fardeau, M.-L., Lascourrèges, J.-F., Joseph, M., Ollivier, B., Aüllo, T., Dequidt, D., Magot, M., and Ranchou-Peyruse, A., 2016, *Desulfotomaculum aquiferis* sp. nov. and *Desulfotomaculum profundi* sp. nov., isolated from a deep natural gas storage aquifer: International Journal of Systematic and Evolutionary Microbiology, v. 66, no. 11, p. 4329–4338, accessed January 2018 at https://doi.org/10.1099/ijsem.0.001352.

Blondes, M.S., Gans, K.D., Engle, M.A., Kharaka, Y.K., Reidy, M.E., Saraswathula, V., Thordsen, J.J., Rowan, E.L., and Morrissey, E.A., 2018, U.S. Geological Survey National Produced Waters Geochemical Database (ver. 2.3, Jan 2018): U.S. Geological Survey data release, accessed January 2018 at https://doi.org/10.5066/F7J964W8.

Brennan, S.T., 2017, Chemical and isotopic evidence for CO_2 charge and migration within Bravo Dome and potential CO_2 leakage to the southwest: Energy Procedia, v. 114, p. 2996–3005, accessed January 2018 at https://doi.org/10.1016/j.egypro.2017.03.1428.

Broadhead, R.F., 1990, Bravo Dome carbon dioxide gas field, *in* Beaumont, E.A., and Foster, N.H., comps., Structural traps I—Tectonic fold traps: Tulsa, Okla., American Association of Petroleum Geologists, p. 213–232, accessed January 2018 at http://archives.datapages.com/data/specpubs/fieldst3/data/a015/a015/0001/0200/0213.htm.

Broadhead, R.F., Mansell, M., and Jones, G., 2009, Carbon dioxide in New Mexico—Geologic distribution of natural occurrences: New Mexico Bureau of Geology and Mineral Resources Open-File Report 514, 131 p.

Buccianti, A., and Pawlowsky-Glahn, V., 2005, New perspectives on water chemistry and compositional data analysis: Mathematical Geology, v. 37, no. 7, p. 703–727, accessed January 2018 at https://doi.org/10.1007/s11004-005-7376-6.

Caporaso, J.G., Kuczynski, J., Stombaugh, J., Bittinger, K., Bushman, F.D., Costello, E.K., Fierer, N., Gonzalez Pena, A., Goodrich, J.K., Gordon, J.I., Huttley, G.A., Kelley, S.T., Knights, D., Koenig, J.E., Ley, R.E., Lozupone, C.A., McDonald, D., Muegge, B.D., Pirrung, M., Reeder, J., Sevinsky, J.R., Turnbaugh, P.J., Walters, W.A., Widmann, J., Yatsunenko, T., Zaneveld, J., and Knight, R., 2010, QIIME allows analysis of high-throughput community sequencing data: Nature Methods, v. 7, no. 5, p. 335–336, accessed January 2018 at https://doi.org/10.1038/nmeth.f.303.

Clark, I.D., and Fritz, P., 1997, Environmental Isotopes in Hydrogeology: Boca Raton, Fla., Lewis Publishers, 342 p.

Clayton, R.N., Friedman, I., Graf, D.L., Mayeda, T.K., Meents, W.F., and Shimp, N.F., 1966, The origin of saline formation waters—1. isotopic composition: Journal of Geophysical Research, v. 71, no. 16, p. 3869–3882, accessed January 2018 at https://doi.org/10.1029/JZ071i016p03869.

Colorado Oil and Gas Conservation Commission, 2018, Colorado Oil and Gas Information System (COGIS): Colorado Oil and Gas Conservation Commission, accessed January 2018 at https://cogcc.state.co.us/data.html#/cogis.

Coplen, T.B., and Kendall, C., 2000, Stable hydrogen and oxygen isotope ratios for selected sites of the US Geological Survey's NASQAN and benchmark surface-water networks: U.S. Geological Survey Open-File Report 00–160, 409 p. [Also available at https://doi.org/10.3133/ofr00160.]

Craddock, W.H., Blondes, M.S., DeVera, C.A., and Hunt, A.G., 2017, Mantle and crustal gases of the Colorado Plateau—Geochemistry, sources, and migration pathways: Geochimica et Cosmochimica Acta, v. 213, p. 346–374, accessed January 2018 at https://doi.org/10.1016/j.gca.2017.05.017.

Craig, H., 1961, Isotopic variations in meteoric waters: Science, v. 133, no. 3465, p. 1702–1703, accessed January 2018 at https://doi.org/10.1126/science.133.3465.1702.

Crossey, L.J., Karlstrom, K.E., Springer, A.E., Newell, D., Hilton, D.R., and Fischer, T., 2009, Degassing of mantle-derived CO_2 and He from springs in the southern Colorado Plateau region—Neotectonic connections and implications for groundwater systems: Geological Society of America Bulletin, v. 121, nos. 7–8, p. 1034–1053. [Also available at https://doi.org/10.1130/B26394.1.]

Cruaud, P., Vigneron, A., Lucchetti-Miganeh, C., Ciron, P.E., Godfroy, A., and Cambon Bonavita, M.-A., 2014, Influence of DNA extraction method, 16S rRNA targeted hypervariable regions, and sample origin on microbial diversity detected by 454 pyrosequencing in marine chemosynthetic ecosystems: Applied and Environmental Microbiology, v. 80, no. 15, p. 4626–4639. [Also available at https://doi.org/10.1128/AEM.00592-14.]

De Cáceres, M., and Legendre, P., 2009, Associations between species and groups of sites—Indices and statistical inference: Ecology, v. 90, no. 12, p. 3566–3574. [Also available at https://doi.org/10.1890/08-1823.1.]

De Filippo, C., Cavalieri, D., Di Paola, M., Ramazzotti, M., Poullet, J.B., Massart, S., Collini, S., Pieraccini, G., and Lionetti, P., 2010, Impact of diet in shaping gut microbiota revealed by a comparative study in children from Europe and rural Africa: Proceedings of the National Academy of Sciences of the United States of America, v. 107, no. 33, p. 14691–14696, accessed January 2018 at https://doi.org/10.1073/pnas.1005963107.

EarthChem, 2018, EarthChem Portal: EarthChem, accessed January 2018 at https://www.earthchem.org/portal.

Egozcue, J.J., Pawlowsky-Glahn, V., Mateu-Figueras, G., and Barceló-Vidal, C., 2003, Isometric logratio transformations for compositional data analysis: Mathematical Geology, v. 35, no. 3, p. 279–300, accessed January 2018 at https://doi.org/10.1023/A:1023818214614.

Engle, M.A., and Blondes, M.S., 2014, Linking compositional data analysis with thermodynamic geochemical modeling—Oilfield brines from the Permian Basin, USA: Journal of Geochemical Exploration, v. 141, p. 61–70, accessed January 2018 at https://doi.org/10.1016/j.gexplo.2014.02.025.

Engle, M.A., and Rowan, E.L., 2013, Interpretation of Na–Cl–Br systematics in sedimentary basin brines—Comparison of concentration, element ratio, and isometric log-ratio approaches: Mathematical Geosciences, v. 45, no. 1, p. 87–101, accessed January 2018 at https://doi.org/10.1007/s11004-012-9436-z.

Engle, M.A., and Rowan, E.L., 2014, Geochemical evolution of produced waters from hydraulic fracturing of the Marcellus Shale, northern Appalachian basin—A multivariate compositional data analysis approach: International Journal of Coal Geology, v. 126, p. 45–56, accessed January 2018 at https://doi.org/10.1016/j.coal.2013.11.010.

Freedman, A.J.E., Tan, B., and Thompson, J.R., 2017, Microbial potential for carbon and nutrient cycling in a geogenic supercritical carbon dioxide reservoir: Environmental Microbiology, v. 19, no. 6, p. 2228–2245, accessed January 2018 at https://doi.org/10.1111/1462-2920.13706.

Geyh, M., D'Amore, F., Darling, G., Paces, T., Pang, Z., and Šilar, J., 2001, Groundwater—Saturated and unsaturated zone, v. IV *of* Environmental isotopes in the hydrological cycle—Principles and applications: Vienna, International Atomic Energy Agency Water Resources Programme., p. 311–424.

Gilfillan, S.M.V., Ballentine, C.J., Holland, G., Blagburn, D., Lollar, B.S., Stevens, S., Schoell, M., and Cassidy, M., 2008, The noble gas geochemistry of natural CO_2 gas reservoirs from the Colorado Plateau and Rocky Mountain provinces, USA: Geochimica et Cosmochimica Acta, v. 72, no. 4, p. 1174–1198, accessed January 2018 at https://doi.org/10.1016/j.gca.2007.10.009.

Gilfillan, S.M.V., Lollar, B.S., Holland, G., Blagburn, D., Stevens, S., Schoell, M., Cassidy, M., Ding, Z., Zhou, Z., Lacrampe-Couloume, G., and Ballentine, C.J., 2009, Solubility trapping in formation water as dominant CO_2 sink in natural gas fields: Nature, v. 458, no. 7238, p. 614–618, accessed January 2018 at https://doi.org/10.1038/nature07852.

González, J.M., Mayer, F., Moran, M.A., Hodson, R.E., and Whitman, W.B., 1997, *Microbulbifer hydrolyticus* gen. nov., sp. nov., and *Marinobacterium georgiense* gen. nov., sp. nov., two marine bacteria from a lignin-rich pulp mill waste enrichment community: International Journal of Systematic and Evolutionary Microbiology, v. 47, no. 2, p. 369–376, accessed January 2018 at https://doi.org/10.1099/00207713-47-2-369.

Grabowski, A., Nercessian, O., Fayolle, F., Blanchet, D., and Jeanthon, C., 2005, Microbial diversity in production waters of a low-temperature biodegraded oil reservoir: FEMS Microbiology Ecology, v. 54, no. 3, p. 427–443, accessed January 2018 at https://doi.org/10.1016/j.femsec.2005.05.007.

Grice, E.A., Kong, H.H., Renaud, G., and Young, A.C., NISC Comparative Sequencing Program, Bouffard, G.G., Blakesley, R.W., Wolfsberg, T.G., Turner, M.L., and Serge, J.A., 2008, A diversity profile of the human skin microbiota: Genome Research, v. 18, no. 7, p. 1043–1050, accessed January 2018 at https://doi.org/10.1101/gr.075549.107.

Ham, B., Choi, B.-Y., Chae, G.-T., Kirk, M.F., and Kwon, M.J., 2017, Geochemical influence on microbial communities at CO_2-leakage analog sites: Frontiers in Microbiology, v. 8, article no. 2203, 15 p., accessed January 2018 at https://doi.org/10.3389/fmicb.2017.02203.

Hardalo, C., and Edberg, S.C., 1997, *Pseudomonas aeruginosa*—Assessment of risk from drinking water: Critical Reviews in Microbiology, v. 23, no. 1, p. 47–75, accessed January 2018 at https://doi.org/10.3109/10408419709115130.

Hartig, K.A., Soreghan, G.S., Goldstein, R.H., and Engel, M.H., 2011, Dolomite in Permian paleosols of the Bravo Dome CO_2 field, U.S.A.—Permian reflux followed by late recrystallization at elevated temperature: Journal of Sedimentary Research, v. 81, no. 4, p. 248–265, accessed January 2018 at https://doi.org/10.2110/jsr.2011.24.

Haszeldine, R.S., Quinn, O., England, G., Wilkinson, M., Shipton, Z.K., Evans, J.P., Heath, J., Crossey, L., Ballentine, C.J., and Graham, C.M., 2005, Natural geochemical analogues for carbon dioxide storage in deep geological porous reservoirs, a United Kingdom perspective: Oil & Gas Science and Technology, v. 60, no. 1, p. 33–49. [Also available at https://doi.org/10.2516/ogst:2005004.]

Hubert, C., and Voordouw, G., 2007, Oil field souring control by nitrate-reducing *Sulfurospirillum* spp. that outcompete sulfate-reducing bacteria for organic electron donors: Applied and Environmental Microbiology, v. 73, no. 8, p. 2644–2652, accessed January 2018 at https://doi.org/10.1128/AEM.02332-06.

Irgens, R.L., 1977, *Meniscus*, a new genus of aerotolerant, gas-vacuolated bacteria: International Journal of Systematic and Evolutionary Microbiology, v. 27, no. 1, p. 38–43, accessed January 2018 at https://doi.org/10.1099/00207713-27-1-38.

Johnson, R.E., 1983, Bravo Dome carbon dioxide area, northeast New Mexico, *in* Fassett, J.E., ed., Oil and gas fields of the Four Corners area v. III: Durango, Colo., Four Corners Geological Society, p. 745–748.

Kakiuchi, M., and Matsuo, S., 1979, Direct measurements of D/H and $^{18}O/^{16}O$ fractionation factors between vapor and liquid water in the temperature range from 10 to 40°C: Geochemical Journal, v. 13, no. 6, p. 307–311. [Also available at https://doi.org/10.2343/geochemj.13.307.]

Kharaka, Y.K., and Hanor, J.S., 2003, Deep fluids in the continents—I. sedimentary basins, chap. 16 *of* Drever, J.I., ed., Surface and ground water, weathering, and soils, v. 5 *of* Holland, H.D., and Turekian, K.K., eds., Treatise on geochemistry: Amsterdam, Elsevier, 48 p.

Kharaka, Y.K., Thordsen, J.J., Kakouros, E., Ambats, G., Herkelrath, W.N., Beers, S.R., Birkholzer, J.T., Apps, J.A., Spycher, N.F., Zheng, L., Trautz, R.C., Rauch, H.W., and Gullickson, K.S., 2010, Changes in the chemistry of shallow groundwater related to the 2008 injection of CO_2 at the ZERT field site, Bozeman, Montana: Environmental Earth Sciences, v. 60, no. 2, p. 273–284, accessed January 2018 at https://doi.org/10.1007/s12665-009-0401-1.

Konter, J.G., and Storm, L.P., 2014, High precision 87Sr/86Sr measurements by MC-ICP-MS, simultaneously solving for Kr interferences and mass-based fractionation: Chemical Geology, v. 385, p. 26–34, accessed January 2018 at https://doi.org/10.1016/j.chemgeo.2014.07.009.

Kostka, J.E., and Luther, G.W., III, 1994, Partitioning and speciation of solid-phase iron in saltmarsh sediments: Geochimica et Cosmochimica Acta, v. 58, no. 7, p. 1701–1710. [Also available at https://doi.org/10.1016/0016-7037(94)90531-2.]

Kuever, J., and Rainey, F.A., 2015, Desulfotomaculum, *in* Whitman, W.B., ed., Bergey's manual of systematics of archaea and bacteria: Hoboken, N.J., John Wiley & Sons, 12 p.

Lambiase, A., 2014, The family *Sphingobacteriaceae*, chap. 72 *of* Rosenberg, E., DeLong, E.F., Lory, S., Stackebrandt, E., and Thompson, F., eds., The prokaryotes—Other major lineages of bacteria and the archaea: Berlin, Springer, p. 907–914.

Lastovica, A.J., On, S.L.W., and Zhang, L., 2014, The family *Campylobacteraceae*, chap. 23 *of* Rosenberg, E., DeLong, E.F., Loy, S., Stackebrandt, E., and Thompson, F., eds., The prokaryotes—Deltaproteobacteria and Epsilonpoteobacteria: Berlin, Springer, p. 307–335.

Leff, J.W., Del Tredici, P., Friedman, W.E., and Fierer, N., 2015, Spatial structuring of bacterial communities within individual Ginkgo biloba trees: Environmental Microbiology, v. 17, no. 7, p. 2352–2361, accessed January 2018 at https://doi.org/10.1111/1462-2920.12695.

Lovell, D., Müller, W., Taylor, J., Zwart, A., and Helliwell, C., 2011, Proportions, percentages, PPM—Do the molecular biosciences treat compositional data right?, chap. 14 *of* Pawlowsky-Glahn, V., and Buccianti, A., eds., Compositional data analysis—Theory and applications: Chichester, England, John Wiley & Sons, p. 191–207.

Lovley, D.R., and Phillips, E.J.P., 1986, Organic matter mineralization with reduction of ferric iron in anaerobic sediments: Applied and Environmental Microbiology, v. 51, no. 4, p. 683–689. [Also available at https://doi.org/10.1128/AEM.51.4.683-689.1986.]

Lucas, S.G., and Hunt, A.P., 1987, Stratigraphy of the Anton Chico and Santa Rosa Formations, Triassic of east-central New Mexico: Journal of the Arizona-Nevada Academy of Science, v. 22, no. 1, p. 21–33.

Luongo, J.C., Barberán, A., Hacker-Cary, R., Morgan, E.E., Miller, S.L., and Fierer, N., 2016, Microbial analyses of airborne dust collected from dormitory rooms predict the sex of occupants: International Journal of Indoor Environment and Health, v. 27, no. 2, p. 338–344, accessed January 2018 at https://doi.org/10.1111/ina.12302.

Madigan, M.T., Martinko, J.M., Stahl, D.A., and Clark, D.P., 2012, Brock biology of microorganisms: San Francisco, Benjamin Cummings, 1,152 p.

Marchandin, H., and Jumas-Bilak, E., 2014, The family *Veillonellaceae*, chap. 35 *of* Rosenberg, E., DeLong, E.F., Lory, S., Stackebrandt, E., and Thompson, F., eds., The prokaryotes—Firmicutes and Tenericutes: Berlin, Springer, p. 433–453.

Mazziotti, M., Henry, S., Laval-Gilly, P., Bonnefoy, A., and Falla, J., 2018, Comparison of two bacterial DNA extraction methods from non-polluted and polluted soils: Folia Microbiologica, v. 63, no. 1, p. 85–92, accessed January 2018 at https://doi.org/10.1007/s12223-017-0530-y.

Oksanen, J., Blanchet, F.G., Kindt, R., Legendre, P., Minchin, P.R., O'Hara, R.B., Simpson, G.L., Solymos, P., Stevens, M.H.H., Szoecs, E., and Wagner, H., 2013, vegan—Community ecology package, version 2(5-2): R Foundation for Statistical Computing software release, accessed January 2018 at https://cran.r-project.org/web/packages/vegan/index.html.

Owen, D.E., 1966, Nomenclature of Dakota Sandstone (Cretaceous) in San Juan Basin, New Mexico and Colorado—GEOLOGICAL NOTES: American Association of Petroleum Geologists Bulletin, v. 50, no. 5, p. 1023–1028, accessed January 2018 at https://doi.org/10.1306/5D25B60F-16C1-11D7-8645000102C1865D.

Palleroni, N.J., 2015, Pseudomonas, *in* Whitman, W.B., ed., Bergey's manual of systematics of archaea and bacteria: Hoboken, N.J., John Wiley & Sons, 56 p.

Parada, A.E., Needham, D.M., and Fuhrman, J.A., 2016, Every base matters—Assessing small subunit rRNA primers for marine microbiomes with mock communities, time series and global field samples: Environmental Microbiology, v. 18, no. 5, p. 1403–1414, accessed January 2018 at https://doi.org/10.1111/1462-2920.13023.

Pawlowsky-Glahn, V., and Buccianti, A., eds., 2011, Compositional data analysis—Theory and applications: Chichester, England, John Wiley & Sons, 378 p. [Also available at https://doi.org/10.1002/9781119976462.]

Peet, K.C., Freedman, A.J.E., Hernandez, H.H., Britto, V., Boreham, C., Ajo-Franklin, J.B., and Thompson, J.R., 2015, Microbial growth under supercritical CO_2: Applied and Environmental Microbiology, v. 81, no. 8, p. 2881–2892, accessed January 2018 at https://doi.org/10.1128/AEM.03162-14.

Peter, A., Lamert, H., Beyer, M., Hornbruch, G., Heinrich, B., Schulz, A., Geistlinger, H., Schreiber, B., Dietrich, P., Werban, U., Vogt, C., Richnow, H.-H., Großmann, J., and Dahmke, A., 2012, Investigation of the geochemical impact of CO_2 on shallow groundwater—Design and implementation of a CO_2 injection test in Northeast Germany: Environmental Earth Sciences, v. 67, no. 2, p. 335–349, accessed January 2018 at https://doi.org/10.1007/s12665-012-1700-5.

Petroleum Recovery Research Center, 2018, New Mexico Produced Water Quality Database version 2: Petroleum Recovery Research Center, New Mexico Institute of Mining and Technology, accessed January 2018 at http://gotech.nmt.edu/gotech/Water/producedwater.aspx.

Pruesse, E., Quast, C., Knittel, K., Fuchs, B.M., Ludwig, W., Peplies, J., and Glöckner, F.O., 2007, SILVA—A comprehensive online resource for quality checked and aligned ribosomal RNA sequence data compatible with ARB: Nucleic Acids Research, v. 35, no. 21, p. 7188–7196, accessed January 2018 at https://doi.org/10.1093/nar/gkm864.

QIIME 2 Development Team, 2017, "Moving pictures" tutorial: QIIME 2 web page, accessed 2017 at https://docs.qiime2.org/2017.11/tutorials/moving-pictures/.

QIIME 2 Development Team, 2018, Data resources: QIIME 2 web page, accessed 2018 at https://docs.qiime2.org/2018.4/data-resources/#.

Quast, C., Pruesse, E., Yilmaz, P., Gerken, J., Schweer, T., Yarza, P., Peplies, J., and Glöckner, F.O., 2013, The SILVA ribosomal RNA gene database project—Improved data processing and web-based tools: Nucleic Acids Research, v. 41, D1, p. D590–D596, accessed January 2018 at https://doi.org/10.1093/nar/gks1219.

R Core Team, 2017, R—A language and environment for statistical computing, version 3.4.3: R Foundation for Statistical Computing software release, accessed January 2018 at https://www.r-project.org/.

Ramirez, K.S., Leff, J.W., Barberán, A., Bates, S.T., Betley, J., Crowther, T.W., Kelly, E.F., Oldfield, E.E., Shaw, E.A., Steenbock, C., Bradford, M.A., Wall, D.H., and Fierer, N., 2014, Biogeographic patterns in below-ground diversity in New York City's Central Park are similar to those observed globally: Proceedings of the Royal Society B, v. 281, no. 1795, 9 p., accessed January 2018 at https://doi.org/10.1098/rspb.2014.1988.

Rochelle, C.A., Pearce, J.M., and Holloway, S., 1999, The underground sequestration of carbon dioxide—Containment by chemical reactions in the deep geosphere: Geological Society, London, Special Publications, v. 157, no. 1, p. 117–129, accessed January 2018 at https://doi.org/10.1144/GSL.SP.1999.157.01.09.

Roth, G., 1983, Sheep Mountain and Dike Mountain fields, Huerfano County, Colorado; a source of CO_2 for enhanced oil recovery, *in* Fassett, J.E., ed., Oil and gas fields of the Four Corners area v. III: Durango, Colo., Four Corners Geological Society, p. 740–744.

Salter, S.J., Cox, M.J., Turek, E.M., Calus, S.T., Cookson, W.O., Moffatt, M.F., Turner, P., Parkhill, J., Loman, N.J., and Walker, A.W., 2014, Reagent and laboratory contamination can critically impact sequence-based microbiome analyses: BMC Biology, v. 12, article no. 87, 12 p., accessed January 2018 at https://doi.org/10.1186/s12915-014-0087-z.

Sathaye, K.J., Hesse, M.A., Cassidy, M., and Stockli, D.F., 2014, Constraints on the magnitude and rate of CO_2 dissolution at Bravo Dome natural gas field: Proceedings of the National Academy of Sciences of the United States of America, v. 111, no. 43, p. 15332–15337, accessed January 2018 at https://doi.org/10.1073/pnas.1406076111.

Shannon, C.E., 1948, A mathematical theory of communication: The Bell System Technical Journal, v. 27, no. 3, p. 379–423. [Also available at https://doi.org/10.1002/j.1538-7305.1948.tb01338.x.]

Shelton, J.L., DeVera, C.A., Morrissey, E.A., Akob, D., Andrews, R., Mumford, A., Brennan, S., and Plampin, M., 2018, Microbiology of the greater Bravo Dome region: U.S. Geological Survey data release, https://doi.org/10.5066/F76M361R.

Shelton, J.L., Engle, M.A., Buccianti, A., and Blondes, M.S., 2018, The isometric log-ratio (ilr)-ion plot—A proposed alternative to the Piper diagram: Journal of Geochemical Exploration, v. 190, p. 130–141. [Also available at https://doi.org/10.1016/j.gexplo.2018.03.003.]

Shelton, J.L., McIntosh, J.C., Hunt, A.G., Beebe, T.L., Parker, A.D., Warwick, P.D., Drake, R.M., II, and McCray, J.E., 2016, Determining CO_2 storage potential during miscible CO_2 enhanced oil recovery—Noble gas and stable isotope tracers: International Journal of Greenhouse Gas Control, v. 51, p. 239–253. [Also available at https://doi.org/10.1016/j.ijggc.2016.05.008.]

Sierra-Garcia, I.N., Dellagnezze, B.M., Santos, V.P., Chaves, M.R.B., Capilla, R., Santos Neto, E.V., Gray, N., and Oliveira, V.M., 2017, Microbial diversity in degraded and non-degraded petroleum samples and comparison across oil reservoirs at local and global scales: Extremophiles, v. 21, no. 1, p. 211–229, accessed January 2018 at https://doi.org/10.1007/s00792-016-0897-8.

Stackebrandt, E., 2014, The family *Eubacteriaceae*, chap. 8 *of* Rosenberg, E., DeLong, E.F., Lory, S., Stackebrandt, E., and Thompson, F., eds., The prokaryotes—Firmicutes and Tenericutes: Berlin, Springer, p. 107–108.

Stevens, S.H., 2005, Natural CO_2 fields as analogs for geologic CO_2 storage, chap. 3 *of* Benson, S.M., ed., Geologic storage of carbon dioxide with monitoring and verification, v. 2 *of* Carbon dioxide capture for storage in deep geologic formations—Results from the CO_2 capture project: Oxford, England, Elsevier, p. 687–697.

Stevens, S.H., Pearce, J.M., and Rigg, A.A.J., 2001, Natural analogs for geologic storage of CO_2—An integrated global research program, *in* Proceedings of the First National Conference of Carbon Sequestration, Washington, D.C., May 14–17, 2001: Morgantown, W.Va., U.S. Department of Energy, National Energy Technology Laboratory, 12 p.

Stover, C.K., Pham, X.Q., Erwin, A.L., Mizoguchi, S.D., Warrener, P., Hickey, M.J., Brinkman, F.S.L., Hufnagle, W.O., Kowalik, D.J., Lagrou, M., Garber, R.L., Goltry, L., Tolentino, E., Westbrock-Wadman, S., Yuan, Y., Brody, L.L., Coulter, S.N., Folger, K.R., Kas, A., Larbig, K., Lim, R., Smith, K., Spencer, D., Wong, G.K.-S., Wu, Z., Paulsen, I.T., Reizer, J., Saier, M.H., Hancock, R.E.W., Lory, S., and Olson, M.V., 2000, Complete genome sequence of *Pseudomonas aeruginosa* PAO1, an opportunistic pathogen: Nature, v. 406, no. 6799, p. 959–964. [Also available at https://doi.org/10.1038/35023079.]

Su, X.-L., Tian, Q., Zhang, J., Yuan, X.-Z., Shi, X.-S., Guo, R.-B., and Qiu, Y.-L., 2014, *Acetobacteroides hydrogenigenes* gen. nov., sp. nov., an anaerobic hydrogen-producing bacterium in the family *Rikenellaceae* isolated from a reed swamp: International Journal of Systematic and Evolutionary Microbiology, v. 64, no. 9, p. 2986–2991, accessed January 2018 at https://doi.org/10.1099/ijs.0.063917-0.

Sun, B., Cole, J.R., Sanford, R.A., and Tiedje, J.M., 2000, Isolation and characterization of *Desulfovibrio dechloracetivorans* sp. nov., a marine dechlorinating bacterium growing by coupling the oxidation of acetate to the reductive dechlorination of 2-chlorophenol: Applied and Environmental Microbiology, v. 66, no. 6, p. 2408–2413, accessed January 2018 at https://doi.org/10.1128/AEM.66.6.2408-2413.2000.

Sun, L., Toyonaga, M., Ohashi, A., Tourlousse, D.M., Matsuura, N., Meng, X.-Y., Tamaki, H., Hanada, S., Cruz, R., Yamaguchi, T., and Sekiguchi, Y., 2016, *Lentimicrobium saccharophilum* gen. nov., sp. nov., a strictly anaerobic bacterium representing a new family in the phylum *Bacteroidetes*, and proposal of *Lentimicrobiaceae* fam. nov: International Journal of Systematic and Evolutionary Microbiology, v. 66, no. 7, p. 2635–2642, accessed January 2018 at https://doi.org/10.1099/ijsem.0.001103.

Takeuchi, M., and Yokota, A., 1992, Proposals of *Sphingobacterium faecium* sp. nov., *Sphingobacterium piscium* sp. nov., *Sphingobacterium heparinum* comb. nov., *Sphingobacterium thalpophilum* comb. nov. and two genospecies of the genus *Sphingobacterium*, and synonymy of *Flavobacterium yabuuchiae* and *Sphingobacterium spiritivorum*: The Journal of General and Applied Microbiology, v. 38, no. 5, p. 465–482, accessed January 2018 at https://doi.org/10.2323/jgam.38.465.

Tschech, A., and Pfennig, N., 1984, Growth yield increase linked to caffeate reduction in *Acetobacterium woodii*: Archives of Microbiology, v. 137, no. 2, p. 163–167. [Also available at https://doi.org/10.1007/BF00414460.]

U.S. Environmental Protection Agency, 2016, Hydraulic fracturing for oil and gas—Impacts from the hydraulic fracturing water cycle on drinking water resources in the United States: Washington, D.C., U.S. Environmental Protection Agency, EPA–600–R–16–236F, variously paged, accessed January 2018 at https://cfpub.epa.gov/ncea/hfstudy/recordisplay.cfm?deid=332990.

U.S. Geological Survey, 2018, USGS water data for the Nation: U.S. Geological Survey National Water Information System database, accessed January 2018 at https://doi.org/10.5066/F7P55KJN.

Vandieken, V., Knoblauch, C., and Jørgensen, B.B., 2006, *Desulfotomaculum arcticum* sp. nov., a novel spore-forming, moderately thermophilic, sulfate-reducing bacterium isolated from a permanently cold fjord sediment of Svalbard: International Journal of Systematic and Evolutionary Microbiology, v. 56, no. 4, p. 687–690, accessed January 2018 at https://doi.org/10.1099/ijs.0.64058-0.

Walters, W., Hyde, E.R., Berg-Lyons, D., Ackermann, G., Humphrey, G., Parada, A., Gilbert, J.A., Jansson, J.K., Caporaso, J.G., Fuhrman, J.A., Apprill, A., and Knight, R., 2015, Improved bacterial 16S rRNA gene (V4 and V4-5) and fungal internal transcribed spacer marker gene primers for microbial community surveys: mSystems, v. 1, no. 1, article no. e00009-15, 10 p., accessed January 2018 at https://doi.org/10.1128/mSystems.00009-15.

Weon, H.-Y., Kim, B.-Y., Yoo, S.-H., Lee, S.-Y., Kwon, S.-W., Go, S.-J., and Stackebrandt, E., 2006, *Niastella koreensis* gen. nov., sp. nov. and *Niastella yeongjuensis* sp. nov., novel members of the phylum *Bacteroidetes*, isolated from soil cultivated with Korean ginseng: International Journal of Systematic and Evolutionary Microbiology, v. 56, no. 8, p. 1777–1782, accessed January 2018 at https://doi.org/10.1099/ijs.0.64242-0.

Whiticar, M.J., 1999, Carbon and hydrogen isotope systematics of bacterial formation and oxidation of methane: Chemical Geology, v. 161, no. 1–3, p. 291–314, accessed January 2018 at https://doi.org/10.1016/S0009-2541(99)00092-3.

Widdel, F., and Bak, F., 1992, Gram-negative mesophilic sulfate-reducing bacteria, chap. 183 *of* Balows, A., Trüper, H.G., Dworkin, M., Harder, W., and Schleifer, K.-H., eds., The prokaryotes—A handbook on the biology of bacteria—Ecophysiology, isolation, identification, applications: New York, Springer, p. 3352–3378.

Worrall, J., 2004, Preliminary geology of Oakdale Field, northwest Raton Basin, Huerfano County, Colorado: AAPG Search and Discovery Article #20017, 14 p.

Yamada, T., Sekiguchi, Y., Hanada, S., Imachi, H., Ohashi, A., Harada, H., and Kamagata, Y., 2006, *Anaerolinea thermolimosa* sp. nov., *Levilinea saccharolytica* gen. nov., sp. nov. and *Leptolinea tardivitalis* gen. nov., sp. nov., novel filamentous anaerobes, and description of the new classes *Anaerolineae* classis nov. and *Caldilineae* classis nov. in the bacterial phylum *Chloroflexi*: International Journal of Systematic and Evolutionary Microbiology, v. 56, no. 6, p. 1331–1340, accessed January 2018 at https://doi.org/10.1099/ijs.0.64169-0.

Zeikus, J.G., Hegge, P.W., Thompson, T.E., Phelps, T.J., and Langworthy, T.A., 1983, Isolation and description of *Haloanaerobium praevalens* gen. nov. and sp. nov., an obligately anaerobic halophile common to Great Salt Lake sediments: Current Microbiology, v. 9, no. 4, p. 225–233, accessed January 2018 at https://doi.org/10.1007/BF01567586.

Zhou, Z., Ballentine, C.J., Schoell, M., and Stevens, S.H., 2012, Identifying and quantifying natural CO_2 sequestration processes over geological timescales—The Jackson Dome CO_2 Deposit, USA: Geochimica et Cosmochimica Acta, v. 86, p. 257–275, accessed January 2018 at https://doi.org/10.1016/j.gca.2012.02.028.

ISSN 2328-0328 (online)
https://doi.org/10.3133/sir20205037